EXTENDED HEATING ABLATION OF CARBON PHENOLIC AND SILICA PHENOLIC

R. W. Farmer

Air Force Materials Laboratory
Wright-Patterson Air Force Base, Ohio

September 1974

NOTICE

When Government drawings, specifications, or other data are used for any purpose other than in connection with a definitely related Government procurement operation, the United States Government thereby incurs no responsibility nor any obligation whatsoever; and the fact that the government may have formulated, furnished, or in any way supplied the said drawings, specifications, or other data, is not to be regarded by implication or otherwise as in any manner licensing the holder or any other person or corporation, or conveying any rights or permission to manufacture, use, or sell any patented invention that may in any way be related thereto.

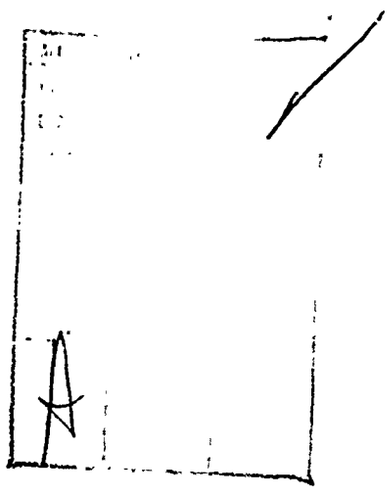

Copies of this report should not be returned unless return is required by security considerations, contractual obligations, or notice on a specific document.

AIR FORCE/56780/25 October 1974 — 100

ic

UNCLASSIFIED

Security Classification

AD/A-000 416

DOCUMENT CONTROL DATA - R & D

(Security classification of title, body of abstract and indexing annotation must be entered when the overall report is classified)

1 ORIGINATING ACTIVITY (Corporate author)	2a. REPORT SECURITY CLASSIFICATION
Air Force Materials Laboratory (MBC) Air Force Systems Command Wright Patterson Air Force Base OH 45433	UNCLASSIFIED 2b. GROUP

3 REPORT TITLE

EXTENDED HEATING ABLATION OF CARBON PHENOLIC AND SILICA PHENOLIC

4 DESCRIPTIVE NOTES (Type of report and inclusive dates)

Final Technical Report September 1972 through January 1973

5 AUTHOR(S) (First name, middle initial, last name)

Farmer, R. W.

6 REPORT DATE	7a. TOTAL NO. OF PAGES	7b. NO. OF REFS
	55	

8a. CONTRACT OR GRANT NO	9a. ORIGINATOR'S REPORT NUMBER(S)
b. PROJECT NO 7340	AFML-TR-74-45
c. Task No. 734001	9b. OTHER REPORT NO(S) (Any other numbers that may be assigned this report)
d.	

10 DISTRIBUTION STATEMENT

Approved for public release; distribution unlimited.

11 SUPPLEMENTARY NOTES	12. SPONSORING MILITARY ACTIVITY
	Air Force Materials Laboratory (MBC) Wright Patterson Air Force Base OH 45433

13 ABSTRACT

An analysis was made of experimental and analytical investigations of the ablation of carbon phenolic and silica phenolic composites under extended heating conditions. Specimens of up to 8.75 sq. in. in area and instrumented with indepth thermocouples were characterized under stepwise pulses of either five minutes (2 steps) or up to 1.4 minutes (to 5 steps) in duration using two air arc heaters. The nominal peak heat load was 35,000 Btu/sq ft. Internal and surface temperatures, recession rates, and recession patterns in the residual char were not anomalous for the two step, low shear (to 2.5 lb/sq ft) runs. Charring-ablator theory indepth and surface temperature responses agreed well with experimental results for a carbon phenolic. For the five step condition with a moderate peak shear (30 lb/sq ft) there was cine film evidence of micromechanical surface removal at late times. Micromechanical effects, by difference, were further consistent with theory. Reliable composite properties were found to be necessary to accurately model extended heating ablation.

DD FORM 1 NOV 65 1473

UNCLASSIFIED

Security Classification

UNCLASSIFIED
Security Classification

KEY WORDS	LINK A		LINK B		LINK C	
	ROLE	WT	ROLE	WT	ROLE	WT
Ablation						
Ablative Materials						
Air Arc Heaters						
Air Arc Heater Characterizations						
Carbon Phenolic						
Heatshields						
Plastics						
Reinforced Plastics						
Silica Phenolic						

ia

UNCLASSIFIED
Security Classification

*U.S.Government Printing Office: 1974 — 657-014/143

AFML-TR-74-45

EXTENDED HEATING ABLATION OF CARBON PHENOLIC AND SILICA PHENOLIC

R. W. Farmer

FOREWORD

This report was prepared by the Thermally Protective Materials Section, Composites and Fibrous Materials Branch, and was initiated under Project 7340, "Nonmetallic Composites and Materials," Task 734001, "Thermally Protective Plastics and Composites." The work was administered under the direction of the Nonmetallic Materials Division, Air Force Materials Laboratory (AFML). The AFML project engineer was Mr. R. Farmer (AFML/MBC). The effort covered the period of September 1972 through January 1973.

This report summarizes and acknowledges an independent, intercomparative, and in-depth analysis of a large body of information resulting from two individual investigations of extended heating ablation. The original work, which includes engineering details as well as empirical observations requiring subjective interpretations, consists of the following:

"Ablative Materials Characterization. Part III. Turbulent High Heating Loads, High Pressure Tests, and High-Modulus Fibrous Composites," B. J. Mitchel and P. J. Roy. AFML-TR-69-188, Part III, December 1970. AF Contract F33615-68-C-1425, Avco Government Products Group.

"Ablative Materials for High Heat Loads. Part I. Environmental Simulation and Materials Characterization," P. W. Juneau, Jr., J. Metzger, L. Markowitz, and F. P. Curtis. AFML-TR-70-95, Part I, June 1970. AF Contract F33615-69-C-1503, General Electric Company.

The reader is referred to these reports (or to their authors) for acquisition of additional specific technical details. This report was submitted by the author February 1974. This technical report has been reviewed and is approved.

T. J. Reinhart Jr

T. J. REINHART, JR., CHIEF
Composite and Fibrous Materials Branch
Nonmetallic Materials Division
Air Force Materials Laboratory

ABSTRACT

An analysis was made of experimental and analytical investigations of the ablation of carbon phenolic and silica phenolic composites under extended heating conditions. Specimens of up to 8.75 sq. in. in area and instrumented with indepth thermocouples were characterized under stepwise pulses of either five minutes (2 steps) or up to 1.4 minutes (to 5 steps) in duration using two air arc heaters. The nominal peak heat load was 35,000 Btu/sq ft. Internal and surface temperatures, recession rates, and recession patterns in the residual char were not anomalous for the two step, low shear (to 2.5 lb/sq ft) runs. Charring-ablator theory indepth and surface temperature responses agreed well with experimental results for a carbon phenolic. For the five step condition with a moderate peak shear (30 lb/sq ft) there was cine film evidence of micromechanical surface removal at late times. Micromechanical effects, by difference, were further consistent with theory. Reliable composite properties were found to be necessary to accurately model extended heating ablation.

TABLE OF CONTENTS

ILLUSTRATIONS

TABLES

SECTION I

INTRODUCTION

Extended heating periods at moderate convective heat fluxes represents a relatively new aerospace environment for efficient charring ablative materials. When environmental regimes with an early thermal soak followed by a second lengthy period became of interest, there was little applicable data for carbon phenolic and silica phenolic. This resultant study was oriented toward definition of any anomalous phenomenology. One postulated case, for example, was the unpredictable formation of relatively weak char regions during early heating with late thermo-mechanically-induced particle loss associated with time-dependent variables as heating rate, pressure, and shear.

As illustrated by Figure 1, two heating pulses were selected to bracket potentially critical response modes. One condition consisted of a long, low heat flux period followed by a step change to a moderately high level. The second environment involved up to five steps with a rapid increase and then a decrease in heat flux. The nominal peak heat load was 35,000 Btu/sq ft for both conditions. The peak char stress was about 12 times larger for the second case as compared to the first one. Table I summarizes nominal values of additional environmental parameters.

The composite specimens, with a cloth layup angle of about 20°, were supported against the rectangular wall of the air arc heater nozzle. The major measurements consisted of internal temperature history, char depth, surface recession, the surface temperature history, and weight loss. The experimental response of the carbon phenolics was compared with the predictions of two transient charring-ablator computer codes.

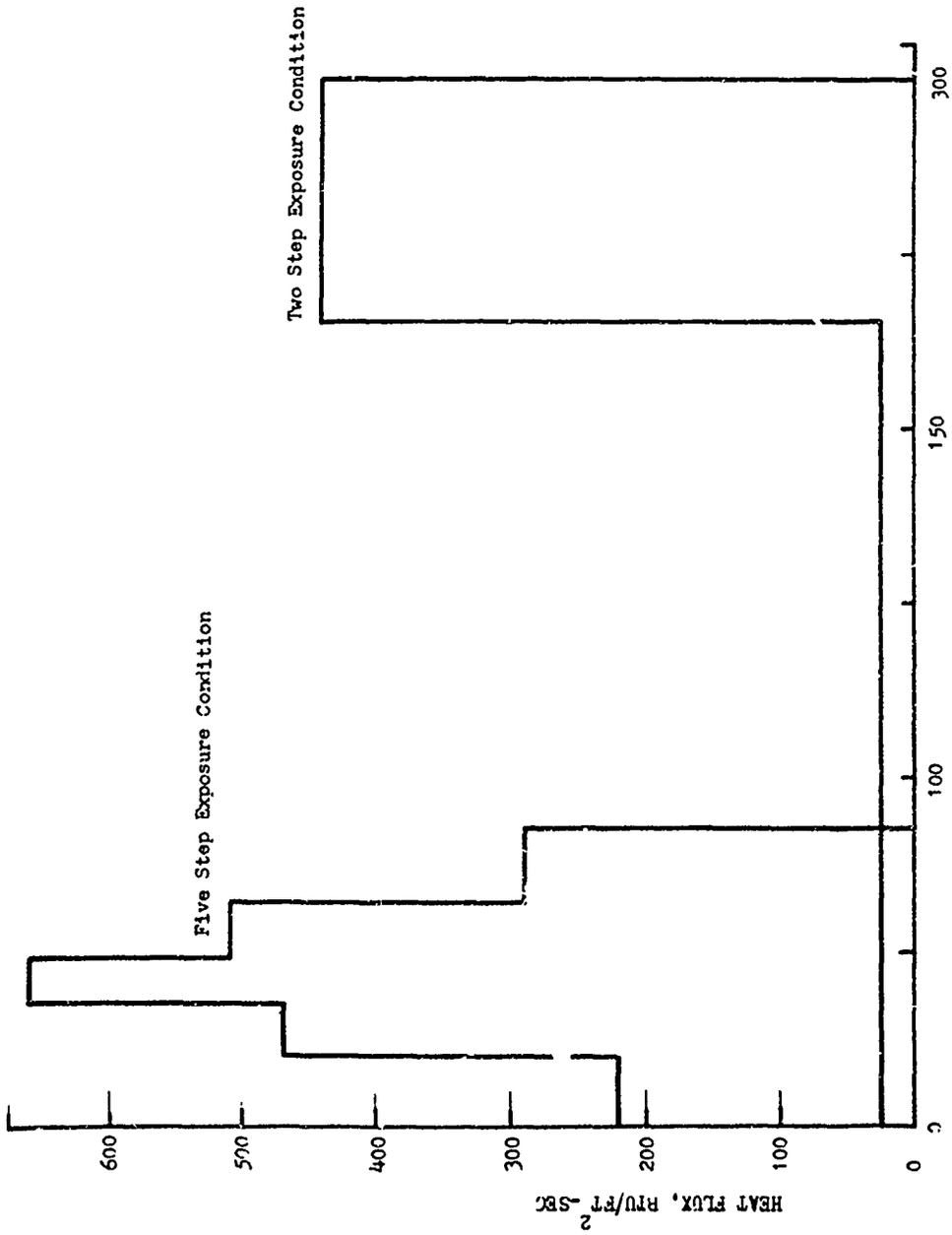

Figure 1. Extended Heating Characterization Environments

TABLE I

NOMINAL ENVIRONMENTAL PARAMETERS

	Two Step		Multiple Step				
Item/Step Number	1	2	1	2	3	4	5
Enthalpy, Btu/lb	5000	5000	1050	3500	6000	3850	1750
Heat Flux, Btu/sq ft-sec	25	440	220	470	660	510	290
Pressure, atm							
Plenum	1	4	0.0	5.3	5.2	5.3	5.5
Specimen	1	1	1.2	1.2	1.2	1.2	1.2
Shear Stress, lb_f/sq ft	0.4	2.5	30	30	30	30	30
Time Interval, sec	230	70	20	15	13	16	21
Total Time, sec	230	300	20	35	48	64	85
Total Heat Load, KBtu/sq ft	5.75	36.6	4.4	11.4	20.0	28.2	34.3

SECTION II

EXPERIMENTAL MATERIALS

Ablative heatshields are frequently prepared by wrapping a prepreg tape on a mandrel under tension at a layup angle near 20°. The tape is made by impregnating bias cut cloth with a phenolic varnish and thermally advancing the resin cure. The mandrel assembly is cured to completion by autoclave or other suitable heating methods under pressure. The complex, biangular configuration of the cloth fibers in a cross-sectional element of the tapewrapped composite may be important in ablative response.

Three composites, codes R1, R2, and R3 were prepared using laboratory autoclave fabrication. Cloth strips cut on a 45° bias angle were impregnated with a phenolic varnish and tacked to an aluminum fixture. An approximate 20° layup angle was maintained with the aid of an end support. The layup was vacuum bagged, thermally advanced, and transferred to an autoclave, cured, removed from the vacuum bag, and postcured. The R6 composite was prepared by high pressure compression molding to achieve maximum density for a thick section. A 20° layup angle was approximated in machining the specimen; a 45° fiber bias angle was not simulated. Table II summarizes fabricational parameters for these composites.

R1, R2, and R3 composite sections were machined for two step exposures. The nominal dimensions were 5 inches in length by 0.5 inches in thickness by 1.75 inches in width. The specimen was prepared by bonding on a 2024-T3 aluminum substructure (chromic acid etched) 0.0625 inches in thickness with HT-435 epoxy-phenolic film adhesive. The composite/plate assembly was clamped for curing for one hour at 350°F. The specimen was instrumented with five 36 AWG Chromel alumel thermocouples and a tungsten reference wire. The thermocouple holes, prepared by axial drilling, were located parallel to the heated surface to minimize heat losses as well as being staggered by about 0.006 inches along the lateral centerline to minimize any interference.

TABLE II

COMPOSITE FABRICATIONAL PARAMETERS

Constituents[a]/Code	R1	R2	R3	R6[e]
Reinforcement	Refrasil	Carbon	Carbon	Carbon
Cloth Type	C-100-43	CCA1-1641	Pluton B1 HP	Pluton B1 HP
Resin Type	USP 95	USP 95	DP 25-10	SC1008
Prepreg Type	FM 5020	FM 5055A	MXC-31HP	MXC31-HP
Prepreg[b]				
Flow, %	17.0	16.1	11.1	6.8
Resin Content, %	27-33	34-36	45-50	44.5
Resin Solids, %				40-45
Volatiles, %	4.0	4.1	6.4	5.5
Cure[c,d]				
Pressure, psi	150	150	150	1000
Time (hr) @ Each Temperature (°F)	2,200°;2,250°; 4,325°	Same as R1	Same as R1	1 hr @ 25° increments, 175° to 350°
Composites				
Density, gm/cc	1.67	1.51	1.43	1.42
Resin Content, %	36.8	35.0	48.5	43.2
Size, inch	12x12x0.60	12x12x0.50	12x12x0.48	6x6x4

[a]C-100-48, CCA1-1641: HITCO., Pluton B1 HP: 3M Co., DP 25-10: Ironsides Resins Co., SC1008: Monsanto Chemical Co., USP 95, FM Prepregs: US Polymeric, Inc., MXC Prepregs: Fiberite Corp., [b]R1, R2, R3: staged @ 15 psi for 1 hr @ 180°F in a vacuum bag. [c]R1, R2, R3: autoclave cure in a vacuum bag. R6: compression molded to stops, cooled under pressure overnight. Postcure for R1, R2, R3: removed from vacuum bag, 4 hr @ 400°F. Postcure for R6: 16 hr @ 200°. 2 hr @ 225°. 2 hr @ 250°, 4 hr @ 275°, 16 hr @ 300°, 4 hr @ 325°. 4 hr @ 350°F. Cooled in oven to 150°F. [e]Reinforcement, resin, and prepreg produced to meet Fiberite Specifications M72201, M74102, and M72251 Rev B high-purity specifications, respectively.

The tungsten wire was located near the specimen center. As summarized by Table III, the nominal thermocouple depths were 0.1, 0.2, 0.3. 0.4, and 0.5 inches, the latter thermocouple being located below the composite in the bond region. The actual depths were estimated by sectioning exposed specimens.

The R6 composite was machined for multiple step exposures. The nominal dimensions for the specimen were 2.50 inches in length by 0.75 inches in thickness by 1.00 inches in width. The specimen was instrumented with four tungsten-rhenium high temperature or Chromel alumel thermocouples at depths consistent with the estimated response of a specimen for a particular exposure sequence. The holes were axially drilled and the depths of the holes were estimated by using a dowel pin as a probe. The thermocouple/sheath assembly was bonded into place. The locations were staggered axially and laterally to minimize any edge heat loss, or mutual interference effects. There were fewer thermocouples near the surface for those specimens intended for a larger number of steps (Table III).

TABLE III

MEAN THERMOCOUPLE DEPTHS*

Run Type/(T/C) Number	1	2	3	4	5
Two Steps	0.104	0.200	0.291	0.404	0.495
Multiple Steps					
1, 1-2	0.076	0.124	0.176	0.226	
1-3	0.121	0.174	0.226	0.276	
1-4	0.173	0.222	0.279	0.329	
3-5	0.174	0.223	0.279	0.329	
3-5	0.222	0.173	0.335	0.376	
1-5	0.224	0.272	0.330	0.376	

*Depths are in inches from the original surface For two step runs, 36 AWG Chromel alumel thermocouples. For multiple step runs, the numbers correspond to the exposure sequence. W+5% Re/W+25% Re thermocouples (beryllia sheaths) to the left of the stepped line; Chromel alumel (alumina sheaths) to the right.

SECTION III

ABLATIVE CHARACTERIZATIONS

1. AIR ARC HEATERS

The arc heater for the two step runs was of the Tandem Gerdien design. As illustrated by Figure 2, air was injected into the two swirl chambers. Most of the air passed through a vortex stabilized arc column, into the plenum chamber, and exhausted through a complex nozzle assembly. The rest of the air was bypassed over the electrodes to remove contaminants and exhausted from the rear of the arc chamber. Two DC generators, connected in parallel, were operated near the maximum rating of 2000 amperes at 1300 volts.

Two step operation was possible by using the assembly illustrated by Figures 3 and 4. A bypass port, which exhausted most of the effluent during the first step of the exposure, was closed by a graphite plug to obtain the more severe second step. The graphite flow deflector was actuated by a reciprocating air cylinder. The variable nozzle, 0.1104 square inches in throat area, provided near supersonic flow with little fluctuation in the arc plenum pressure after closure of the bypass port. Figure 3 further illustrates the variable nozzle instrumentation, specimen installation, and a graphite insulator used to isolate the specimen from the water-cooled copper hardware.

The effluent bulk enthalpy was estimated by an energy balance. Heat flux calibration measurements were made with a water-cooled calorimeter in the specimen position. A heat flux transducer in the variable nozzle, intended for monitoring during the run, was not satisfactory. Therefore, specimen values were estimated using calibration data and the environmental parameters. Pressure histories were measured for the arc and extension plenums and at three stations above the specimen along the variable nozzle wall. Shear stress was nominally evaluated using Reynold's Analogy. Additional arc operational measurements primarily involved the air mass flow rate, cooling water flow rate and temperature

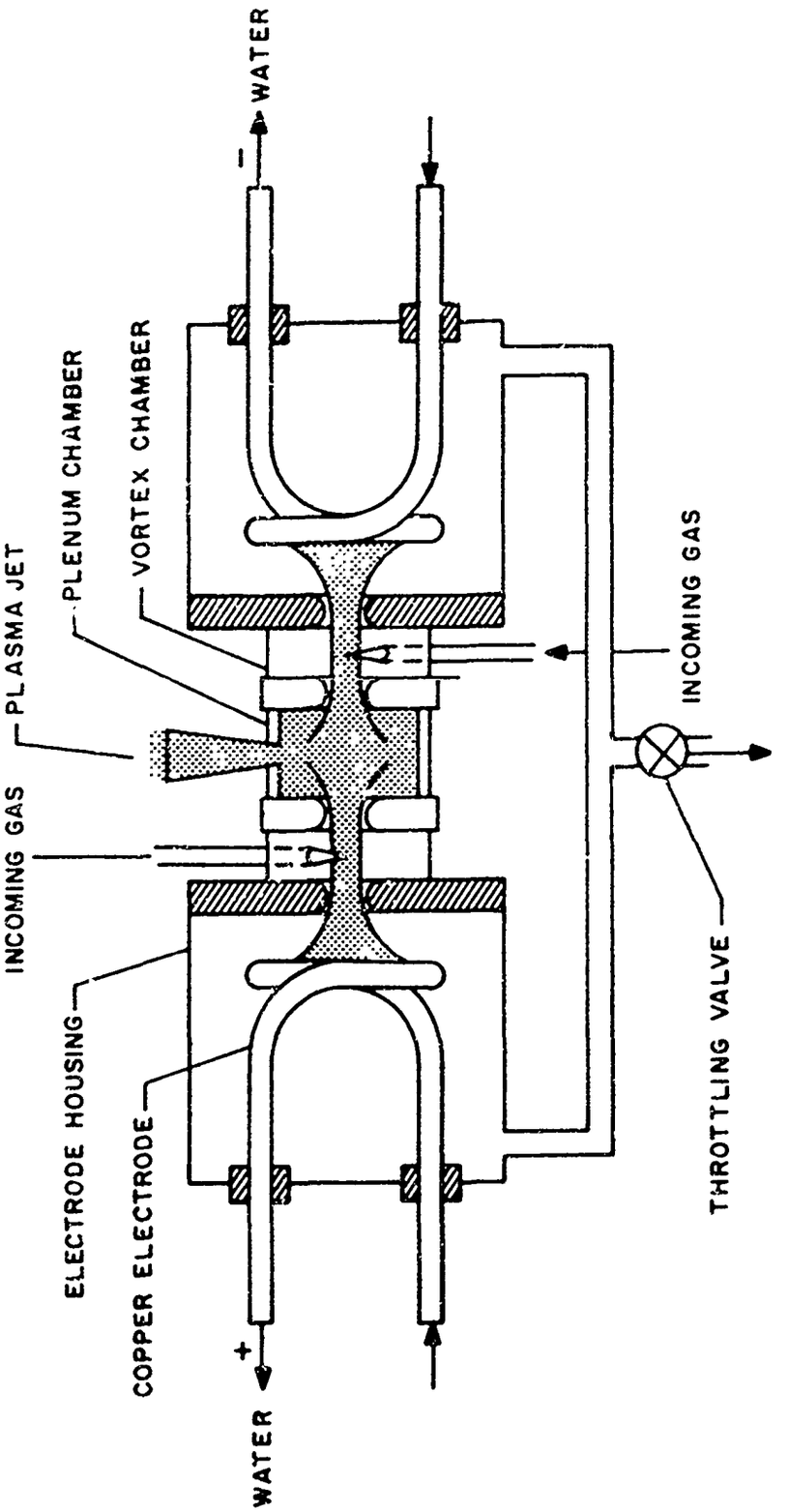

Figure 2. Tandem Electrode Air Arc Heater

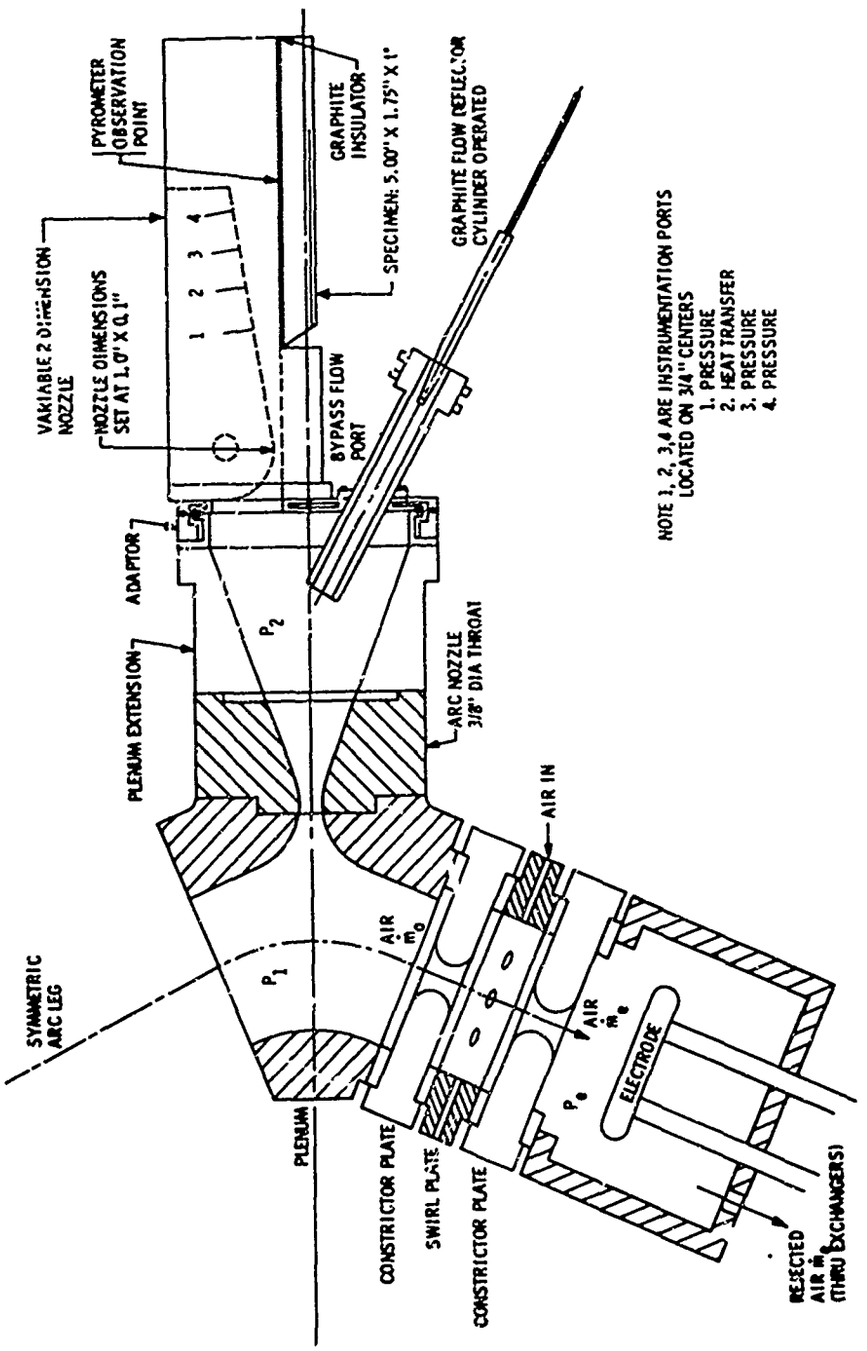

Figure 3. Arc Heater And Specimen Arrangement

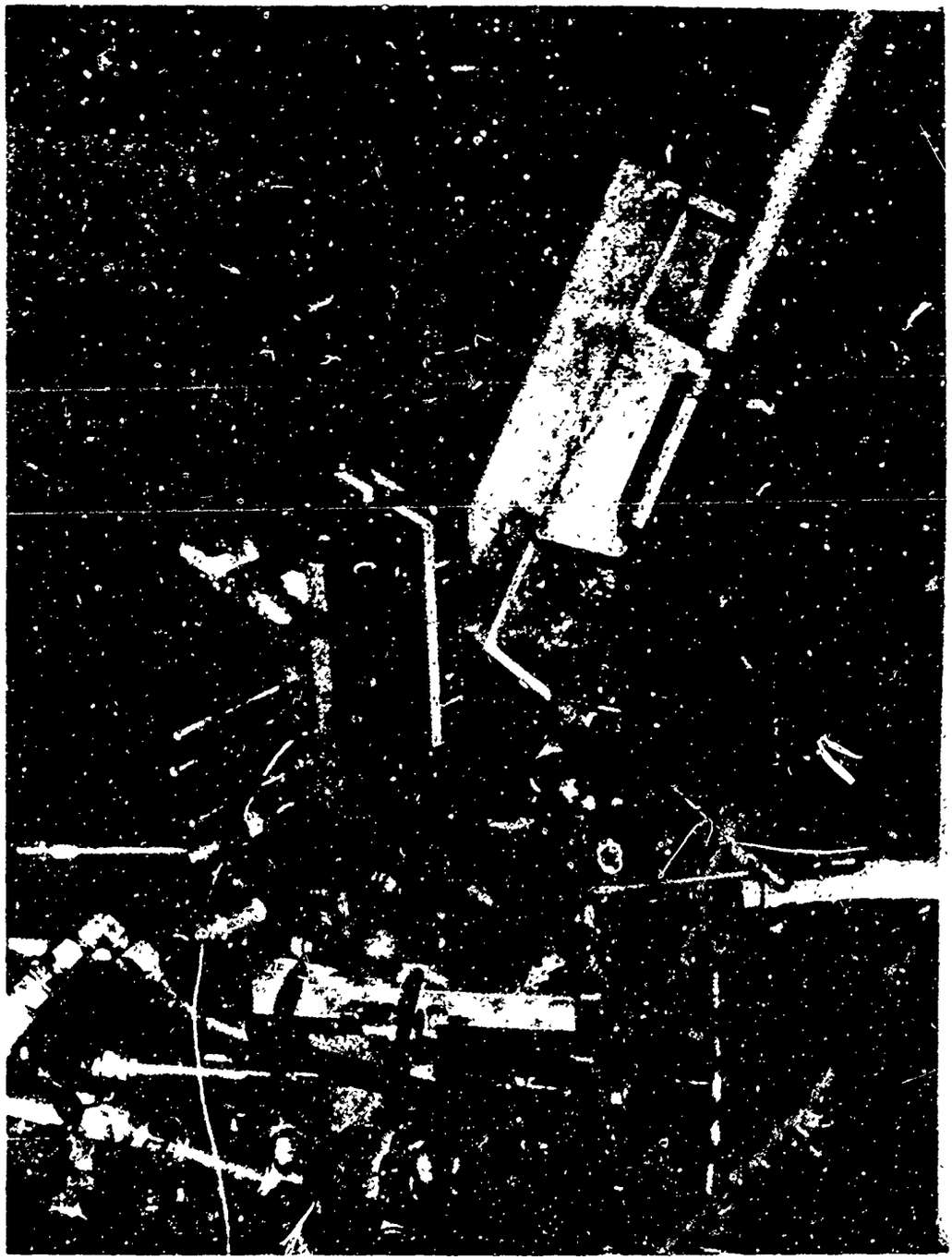

Figure 4. Arc Heater Installation

change, current, and voltage. The continuously recorded parameters generally stabilized at a constant level within a few seconds after run initiation.

Figure 4 is an overall view of the arc, specimen installation, and supporting instrumentation.

The facility for the multiple step exposures essentially consisted of five air arc heaters discharging into a spherical plenum (Figure 5). The effluent exhausted in a direction normal to the four equally spaced arc heads and parallel to the fifth. The power supply consisted of 2080 heavy-duty, 12-volt storage batteries.

The air mass flow rate and the power to each arc head were programmed both sequentially to step change enthalpy and heat flux as well as separately to maintain a nearly constant plenum pressure with proper effluent expansion. The contoured, rectangular nozzle was 1.465 inches in height by 1.000 inch in width at the exit plane. The nominal Mach Number was 1.79. Figure 6 illustrates the specimen installation at a 10° inclination angle. The nozzle and specimen holder was made from copper. Figure 7 is an overall view of the source, specimen installation, and supporting instrumentation.

The effluent bulk enthalpy was estimated from a correlation for sonic mass flow at the nozzle throat, as derived from isentropic flow relationships. The correlation was confirmed by selected enthalpy probe measurements. Heat flux was primarily estimated from correlation curves based upon calibration experiments and theory. The plenum pressure history was recorded and correlated to give a specimen surface pressure. Shear stress was estimated from Reynold's Analogy. The time interval for the steps generally corresponded to a step deflection of an oscillograph record. Steady state current, plenum pressure, and voltage values were generally achieved in less than 0.2 seconds after run or step initiation.

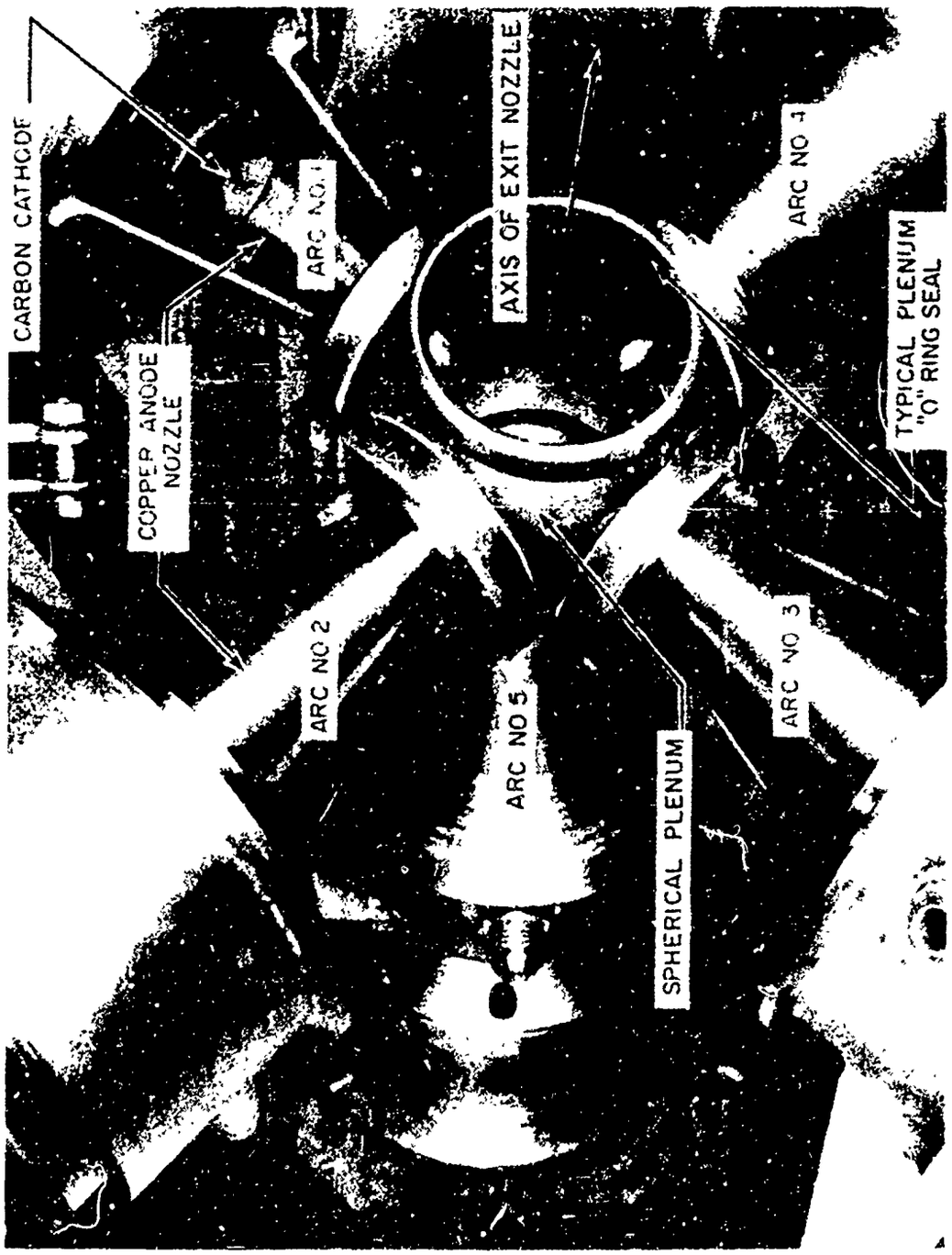

Figure 5. Multiple Electrode Air Arc Heater

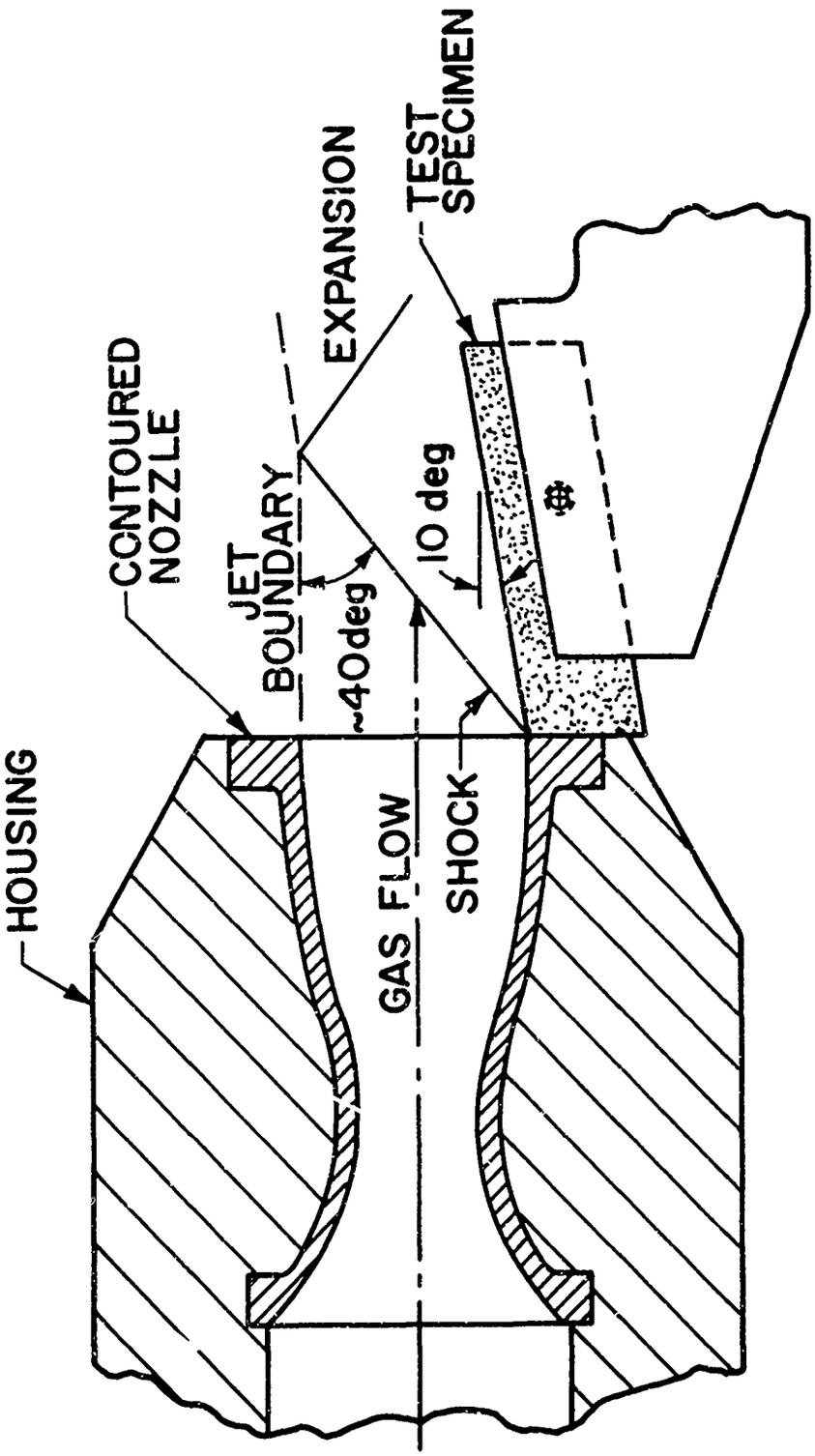

Figure 6. Arc Nozzle And Specimen Arrangement

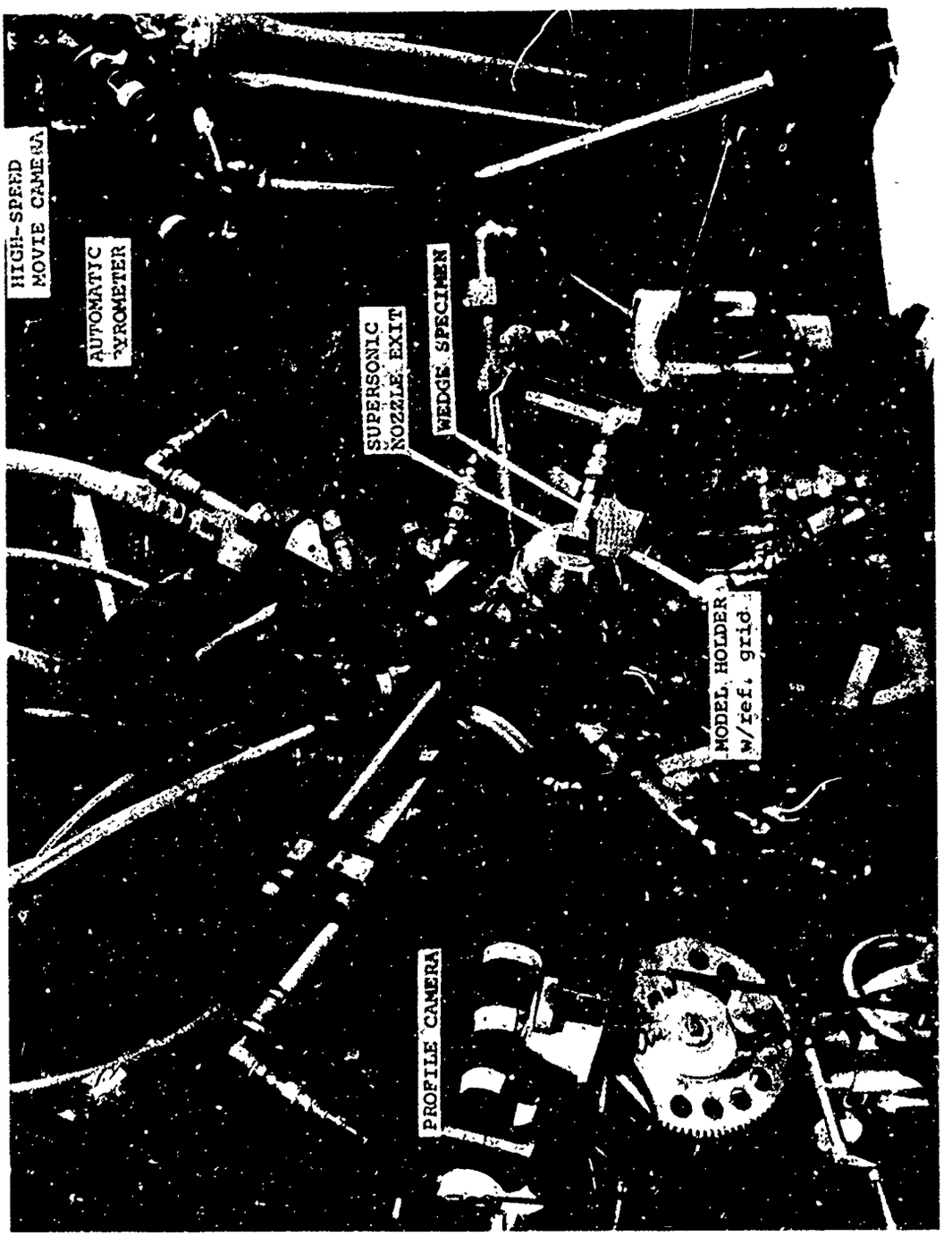

Figure 7. Arc Heater Installation And Instrumentation

2. SPECIMEN MEASUREMENTS

The specimen measurement procedures were not the same for the two types of characterizations consistent with available apparatus, behavioral differences, and data uses. The measurements during exposure did include an in-depth internal temperature history and a surface temperature history at one station. In addition, the surface recession history was obtained by a photographic technique for the strongly transient multiple step runs. Post-test measurement involved local and/or overall char depth, surface recession, and weight loss.

For two step runs, the in-depth thermocouple responses were recorded by an oscillograph. The surface color temperature was recorded by a two-color pyrometer viewing a nominal 0.25 inch diameter area just outside the nozzle exit. The total specimen weight change was obtained by differential weighing. Axial char depth and surface recession profiles were obtained along the center line of a sectioned specimen using a cathetometer. Time lapse 16 mm color photography of the specimen surface during exposure proved unsatisfactory due to camera malfunctions and other difficulties.

Analysis of the widely variable in-depth thermocouple responses for multiple step runs was facilitated by magnetic tape recording, digitization, and computer processing. An oscillograph was also used for data recording. Brightness temperature and total radiation histories were obtained by an infrared pyrometer and thermopile arrangement, respectively. The reference station was on the centerline 1.5 inches from the nozzle exit. The fields of view were 0.13 and 0.33 inches in diameter for the pyrometer and thermopile, respectively. The surface recession history was obtained at the reference station, 1.5 inches from the nozzle, using 35 mm camera film strips made at a 2 second framing rate. The surface recession was generally not uniform over the specimen. Therefore, a 0.5 inch diameter core was removed from the reference station. This core was used for the assessment of specimen thickness and weight changes. In addition, a mean local areal weight change was

calculated as the difference of the average initial areal weight of the specimen and the areal weight of the core. Color 16 mm movies were made of the specimen surface during exposure.

SECTION IV

COMPUTER CODES

Carbon phenolic response was assessed using two charring-ablator computer codes. While similar in many respects, there were differences relating to formulation, modelling, solution, and property definition. Although descriptions of each were beyond the scope of this report, essential features were reviewed for illustrative purposes.

The transient ablation code for the two step runs modelled finite phenolic resin pyrolysis kinetics, gas phase chemical reactions, and temperature-dependent thermophysical properties. These mechanisms were considered potentially significant for the thick chars found for this environment. The one-dimensional in-depth heat balance included chemical reactions, conduction, gas phase storage, and solid storage with phenolic pyrolysis kinetics being expressed as an Arrhenius-type correlation. There was zero net conduction at the substructure boundary. The surface energy solution balanced convective heating, pyrolysis gas blockage in the boundary-layer, and surface radiation. Recession rate was represented by a (Knudsen-Langmuir)-type correlation with three empirical coefficients. The governing equations for the code were solved simultaneously at selected in-depth nodes in real time. As the code was terminated,if an incremental solution was not calculated within specific accuracy limits, a modification was necessary to reduce computational time increments in the vicinity of the step change.

The input materials properties were nominal values representative of the R2 composite and typical for this materials class (Table IV). The inputs included both conventionally measured thermophysical properties as well as experimentally measured and estimated data empirically accounting for gas phase chemical reactions and recession rate. The environmental definition inputs included both nominal and adjusted values of the environmental parameters. The adjusted values were based upon an analysis of the experimental data.

TABLE IV

REPRESENTATIVE ABLATION AND COMPOSITE PROPERTIES

	R2/R3 Class[a]		R6[b]			R6 Class[c]		
	Char Zone	Virgin Zone	Char Zone	Virgin Zone	Pyrolysis Gas	Char Zone	Virgin Zone	Pyrolysis Zone
Density, lb/cu ft	74.0	90.4	73.6	92.0		68.4	91.2	
Emittance	0.85		0.7	0.7				
Heat of Char Combustion, KBtu/lb			-4.36/-4.60[d]		-1.8/+3.0[d]			
Heat of Pyrolysis KBtu/lb				0.48		0/0[d]	0.205	
Resin Pyrolysis Temperature. °F				540			1000	
Specific Heat, Btu/lb-°F	0.22 to 0.55		0.45	0.25	0.80	0.35	0.35	0.44
Specific Heat Temperature Range, °F	0° to 4550°							
Thermal Conductivity, Btu/hr-ft-°F	0.34 to 1.60		0.40 to 2.56	0.46		1.0	0.44	
Thermal Conductivity Temperature Range, °F	0° to 4550°		540° to 4540°					

[a]Representative values for R2/R3 class of composites. [b]Based upon a nonlinear regression analysis of steady-state ablation data for R6. [c]Typical experimental or estimated data for R6-type composites. [d]For 4040°/5840°F, respectively, at 1 atm pressure.

The code applied to multiple run analysis considered blowing, combustion (gas, solid), the heat of resin pyrolysis, storage (gas, solid), surface radiation, temperature-dependent char thermal conductivity, and thermal conduction in depth (gas, solid). Phenolic pyrolysis was expressed in terms of a step change from virgin material to char at a constant pyrolysis temperature. Surface recession was assumed to result from diffusion-limited oxidation and removal of the char. The rate balance considered blocking, combustion (gas, solid), the oxygen flux, and the pyrolytic gas flux. The equations were solved by a technique well suited to examine the various experimental exposure sequences. Essentially, the relations were transformed into a moving coordinate system, further transformed to increase the grid-point density in regions of high temperature, and formulated into an implicit finite-difference scheme for simultaneous solutions at each step. Small steps were not required when the char front was near the surface.

The input properties for the R6 composite were determined by a nonlinear regression analysis of internal and surface temperature data. This widely used technique was applied to an R6 specimen exposed in a more severe environment to achieve steady-state ablation. These properties were considered adequate for a first assessment in that the maximum difference between the experimental temperatures and temperatures calculated using the code, derived properties, and nominal environmental parameters did not exceed about 200°F at any of four depths or 450°F at the surface. Table IV summarizes the properties obtained from the regression analysis as well as other data measured by various techniques for composites similar to R6 with respect to type of reinforcement and resin. The environmental inputs for the analysis of the response to multiple step heating corresponded to the nominal environmental parameters for that exposure sequence.

SECTION V

RESULTS AND DISCUSSION

1. TWO STEP EXPOSURES

The carbon phenolic composites R2 and R3 were exposed to the two step condition. The approximate mean char thicknesses for R2/R3 were 0.28/0.21 inches and the corresponding mean recession was 0.11/0.06, respectively (Table V). As illustrated by Figure 8, there were differences in the internal char profiles and external surface patterns for these two composites.

There was considerable recession in the leading edge region for R3. An early high recession rate may have been self-aggravating in promoting local environmental changes and a higher than normal recession rate. The excessive ejected material may have further reduced downstream recession. For R2, although the surface was considerably smoother, a higher overall char irregularity was found than for R3.

The char profile unevenness was partially a result of the surface irregularity and porosity. This was due to the station to station measurement technique bias of the char depth data in that the char thickness was taken as the depth difference between the surface and char interface.

There were large differences in the internal temperature responses of R2 and R3 (Figures 9 and 10). R2 provided considerably superior insulative ability during the first step. The temperatures increased rapidly for both specimens after the onset of second step heating.

Ths surface temperature history consisted of a nearly steady value near 2030°R for the first heating pulse with a step change for the second (Figure 11). The surface temperature for R2 averaged a negligible 120°F higher than for R3 for the first step. While the temperature stabilized near 4070°R for R3 for the second pulse, there was a saddle-like fall-off

TABLE V

SPECIMEN DIMENSIONAL CHANGES

Two Step Exposures[a]									
Code	Composite Type	Thickness, inch	Mean Thickness, inch	Recession, inch	Mean Recession, inch	Char Thickness, inch	Mean Char Thickness, inch	Initial Weight, gm	Weight Loss, gm
R1	S/P	0.553-0.570	0.555	0.017-0.102[b]	0.077[b]	0.189-0.274	0.200	146.967	10.695
R2	C/P	0.574-0.578	0.574	0.044-0.087	0.056	0.181-0.282	0.280	133.559	15.494
R3	C/P	0.550-0.558	0.558	0.068-0.182	0.108	0.147-0.231	0.210	124.970	21.334

Multiple Step Exposures			Specimen Values[c]			Core Values[d]			Areal Weight Changes, lb/Sq.ft	
Specimen Number	Step Sequence	Density, lb/cu ft	Thickness, inch	Weight, gm	Weight Loss, gm	Diameter, inch	Weight, gm	Recession, inch	Core	Specimen
1	1	91.1	0.750	44.8	1.1	0.500	3.481	-0.015	0.07	0.14
2	1-3	91.4	0.749	44.9	7.5	--[e]	--[e]	0.031	--[e]	0.95
3	1-3	91.6	0.750	45.0	10.8	0.501	2.770	0.083	1.25	1.37
4	1-3	91.2	0.749	44.8	13.9	0.501	2.428	0.124	1.77	1.77
5	1-4	91.3	0.751	45.0	17.0	0.501	2.115	0.212	2.30	2.16
6	3-5	91.0	0.750	44.7	11.3	0.502	2.672	0.140	1.38	1.44
7	3-5	91.6	0.750	45.0	13.3	0.501	2.480	0.145	1.72	1.69
8	1-6	91.1	0.750	44.8	22.1	0.501	1.568	0.340	3.13	2.81

[a]Thickness includes adhesive bond and aluminum substructure. Char thickness and recession ranges exclude the station adjacent to the nozzle. [b]Mean silica layer thickness was 0.014 inches. [c]Initial values before thermocouple installation; residual values determined after lead wire and adhesive removal. [d]Core drilled at centerline reference station 1.50 inches from the nozzle exit. [e]Core fractured while drilling.

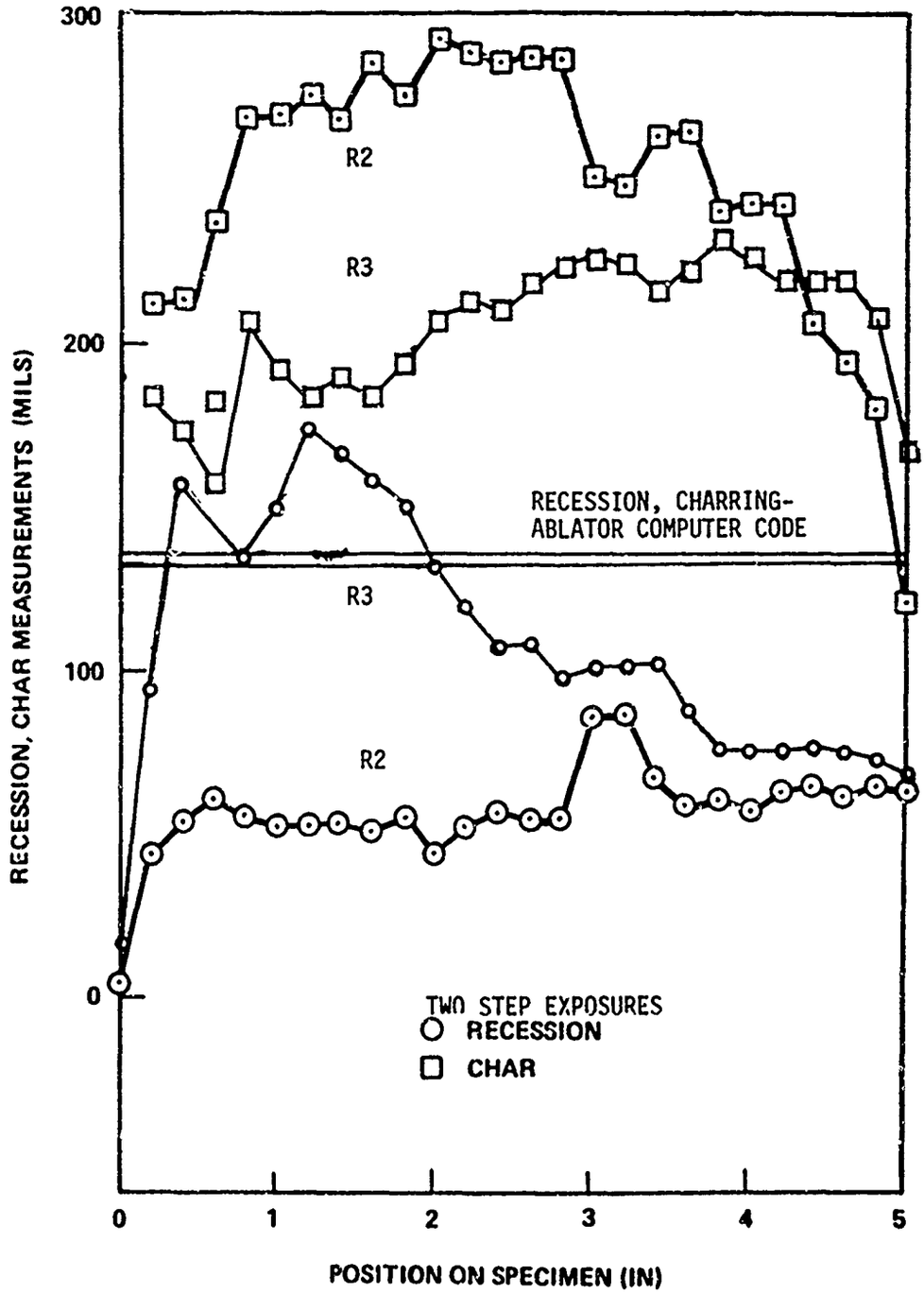

Figure 8. Char Depth And Surface Recession For Carbon Phenolics

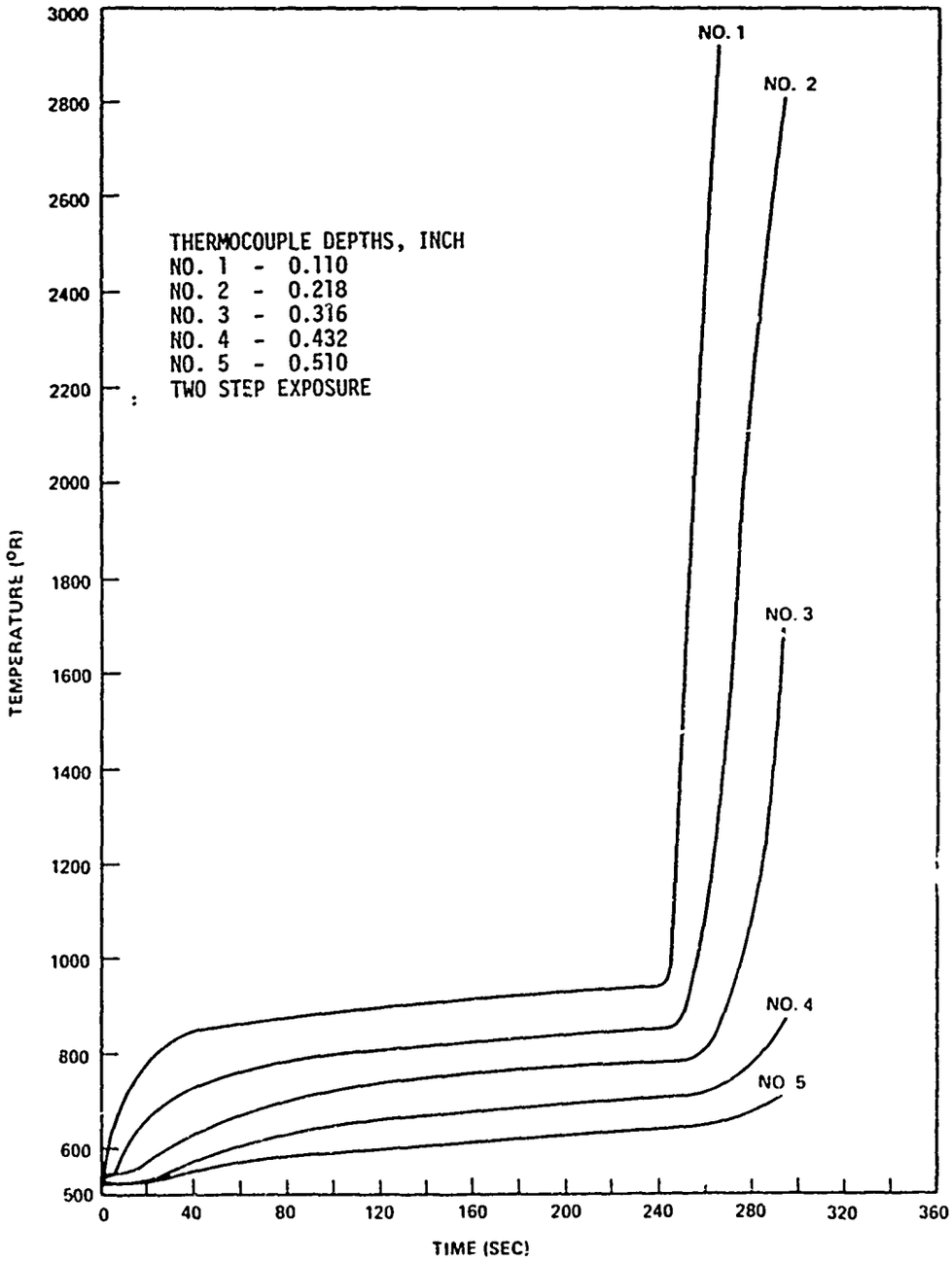

Figure 9. Internal Temperature Histories For R2 Carbon Phenolic

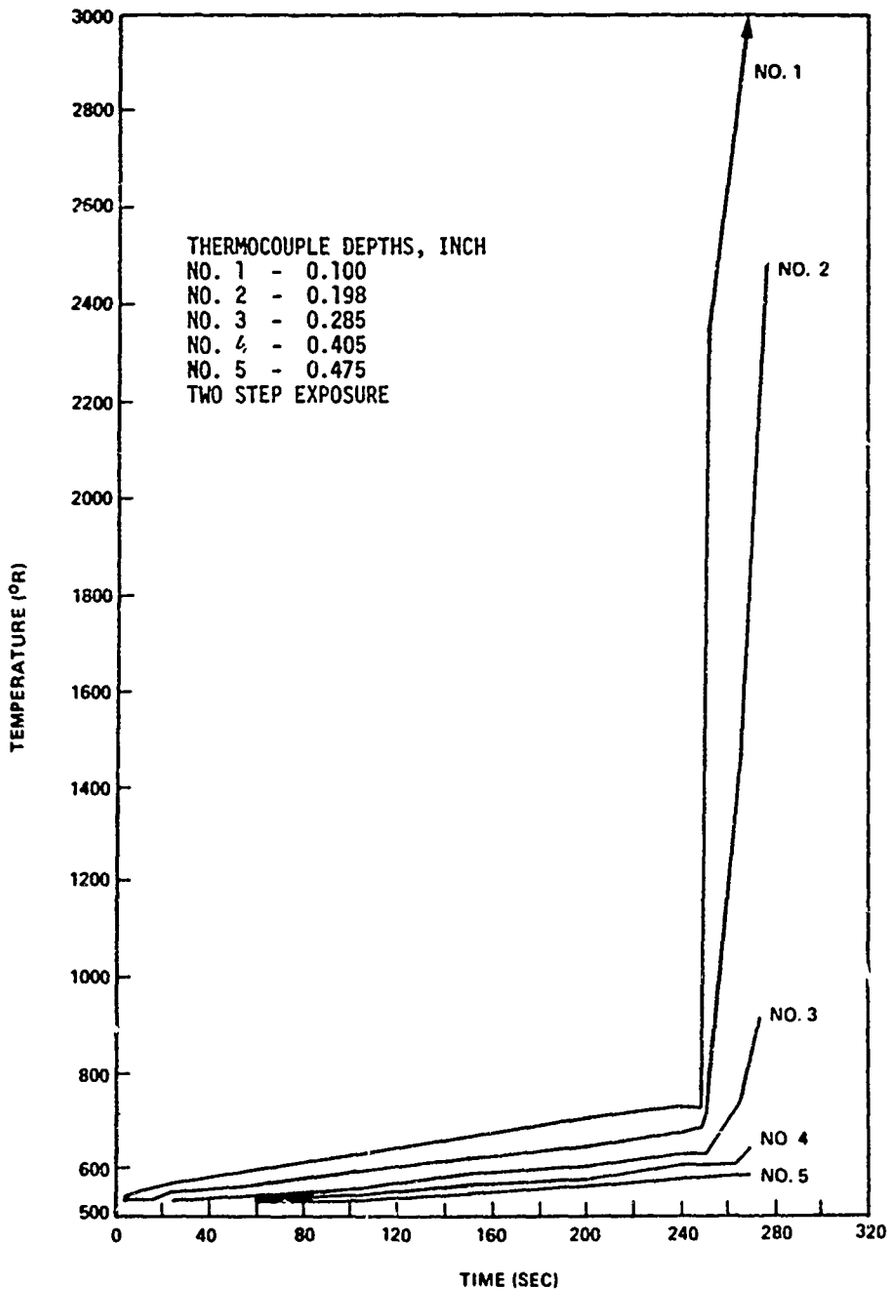

Figure 10. Internal Temperature Histories For R3 Carbon Phenolic

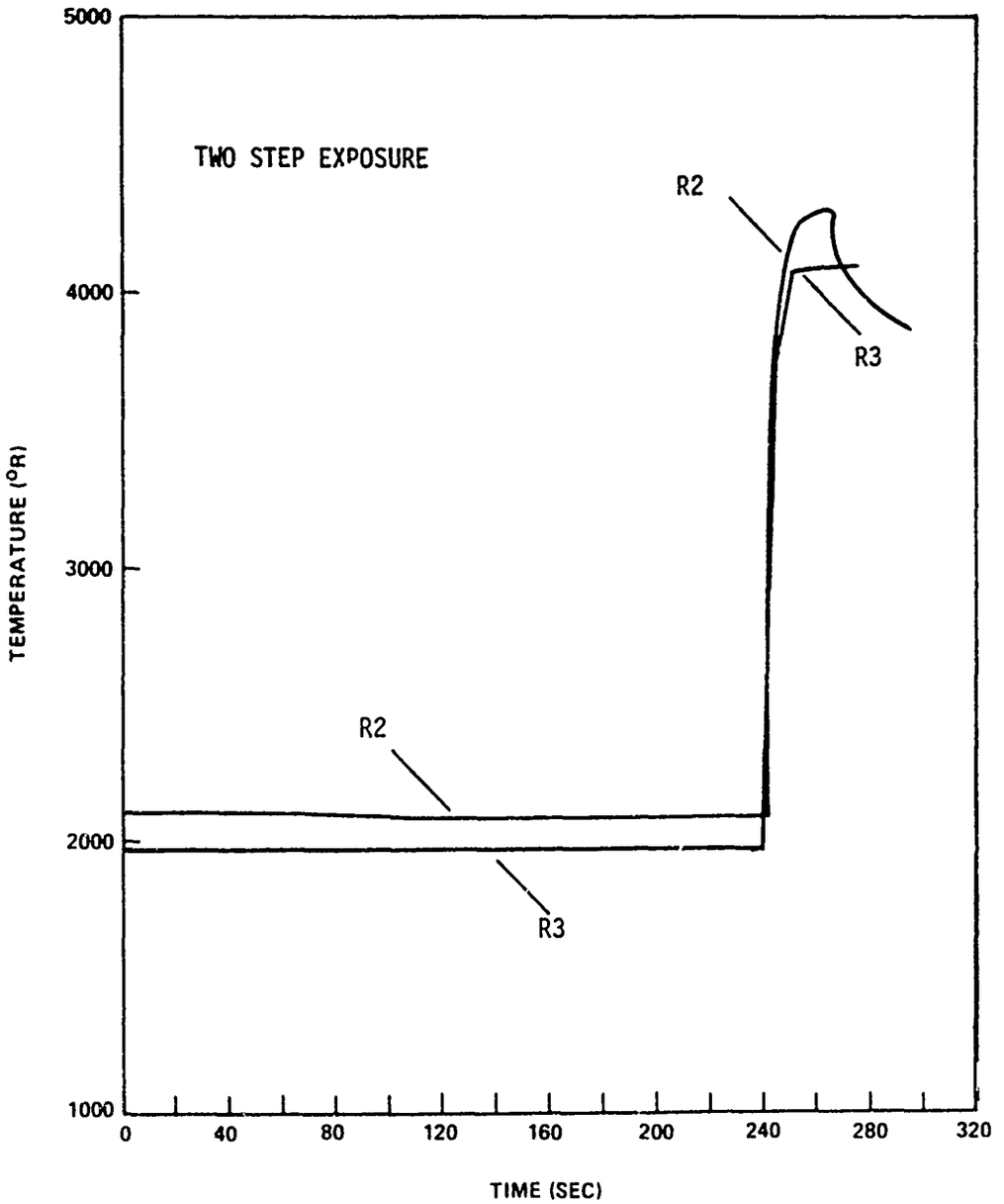

Figure 11. Surface Temperature Histories For Carbon Phenolics

for the R2 specimen. For the measured data a constant grey body condition was assumed and the results were reported as nominally true values. This was considered to be a reasonable first approximation in that a ±25% uncertainty for a representative emittance of 0.8 resulted in a temperature uncertainty of only about ±6%.

Although achieved in later efforts, the nominal environmental parameters were not met in the early work reported herein due to equipment and instrumentation limitations (Tables I and VI). In general, the heat flux and heat load for the second step as well as the enthalpy was low. Further, the exposure times were longer and more brief than nominal for the first and second steps, respectively. A higher plenum pressure was used experimentally and sub-atmospheric flow expansion was found in several cases.

The heat flux was lower for R2 as compared to R3 and the enthalpy was lower for R3 relative to R2 (Table VI). The highest plenum pressure, plenum extension pressure, and nozzle pressure at the three stations was generally found for the R3 run. There was no consistent dependency of charring, recession, in-depth response, or surface temperature on the differences in these environmental parameters for the two specimens.

For silica phenolic (Code R1), the approximate mean char depth and corresponding mean recession was 0.200 and 0.077 inches, respectively (Table V). Figure 12 illustrates the profiles for the char, surface recession, and a residual layer resulting from melting of the silica cloth. The mean layer thickness was about 0.014 inches. There was considerable and uneven charring near the leading edge. The recession peaked in the central region of the specimen. The nominal environmental parameters were not readily obtained experimentally (Table I and VI).

TABLE VI

EXPERIMENTAL RESULTS - TWO STEP EXPOSURES

Item/Code	R1	R2	R3
Composite Type	S/P	C/P	C/P
Environment			
Enthalpy, Btu/lb	4540	4900	4486
Heat Flux, Btu/sq ft-sec	21.4/276	23.0/255	21.0/312
Pressure, atm			
Plenum	6.7	5.6	6.8
Extension	1.0/4.2	1.0/4.0	0.95/4.0
Nozzle, St 1	1.0/2.6	1.0/0.88	1.0/1.2
3	1.0/2.0	0.96/0.75	0.96/1.1
4	1.0/---	1.0/0.61	0.95/0.95
Time, sec	243/48	242/51	243/52
Total Heat Load, KBtu/sq ft	5.20/13.2	5.56/13.0	5.10/16.2
Response			
Initial Thickness inch[a]	0.555	0.574	0.558
Recession, inch[b]	0.077	0.056	0.108
Surface Temperature, ^{o}R	1980/4020	2090/4040	1970/4070

[a] Thickness includes adhesive bond and aluminum substructure. [b] Mean recession value.

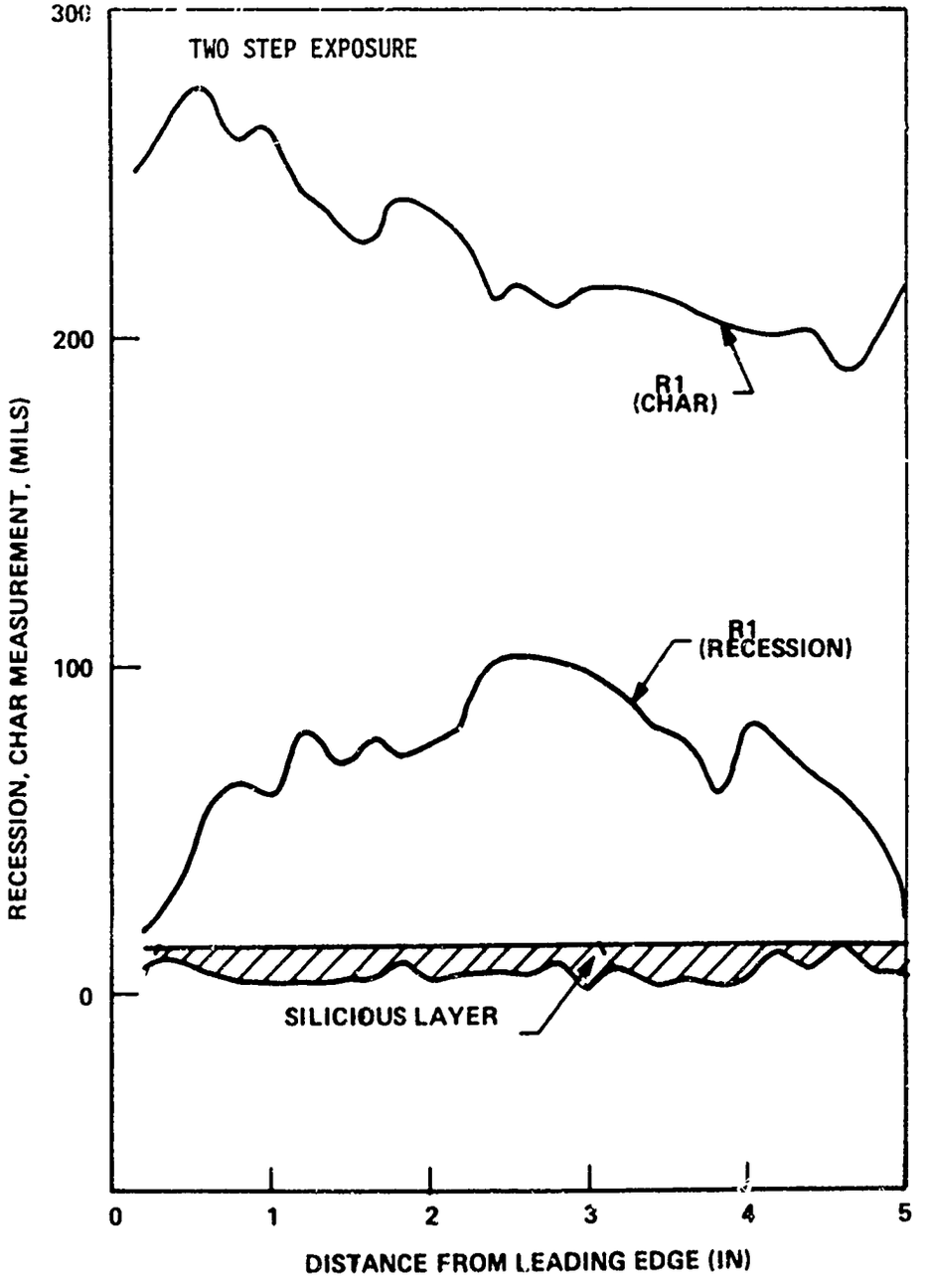

Figure 12. Char Depth And Surface Recession For R1 Silica Phenolic

The internal temperature histories for the R1 run revealed unexpected high internal heating (Figure 13). Even considering the differences in actual thermocouple depths, the temperatures exceeded those found at any given time for R2 and R3 (Figures 9 and 10). Figure 13 represents an inexplicable "worst case" in that less severe thermal gradients were found for two incompleted runs for this composite. In addition, less internal heating was observed for another silica phenolic composite (C-100-48/DP 25-10) of comparable composition. The recession and second step surface temperatures were higher for the second material consistent with a higher heat flux for this step. For the second silica phenolic composite, the internal temperature histories were similar in form to that of the carbon phenolic composite R3. The silica phenolic composite temperatures, however, were about 100°F lower at the first thermocouple depth with a smaller difference being observed at greater depths.

The surface temperatures were nearly identical for the R1 and R3 composites for the first step and the difference did not exceed about 400°F for the second (Figure 14). As for the carbon phenolics, the R1 color temperatures were taken as true values by assuming a grey body condition as a first approximation.

A charring-ablation computer code was used to assess the response of a representative carbon phenolic in a nominal two step environment. As the thermophysical properties were not available for the R2 and R3 composites, the major materials property inputs were taken as being similar to those of Table IV. The selected values had the additional advantage of confirmation in other work. In addition to the properties uncertainty, which was most important with respect to in-depth charring and temperatures, the time-resolved environmental parameters were not available for each run. It was possible, however, to average extensive data to provide mean values of enthalpy, heat flux, and pressure. The uncertainty in these parameters was significant primarily with respect to recession and surface temperature.

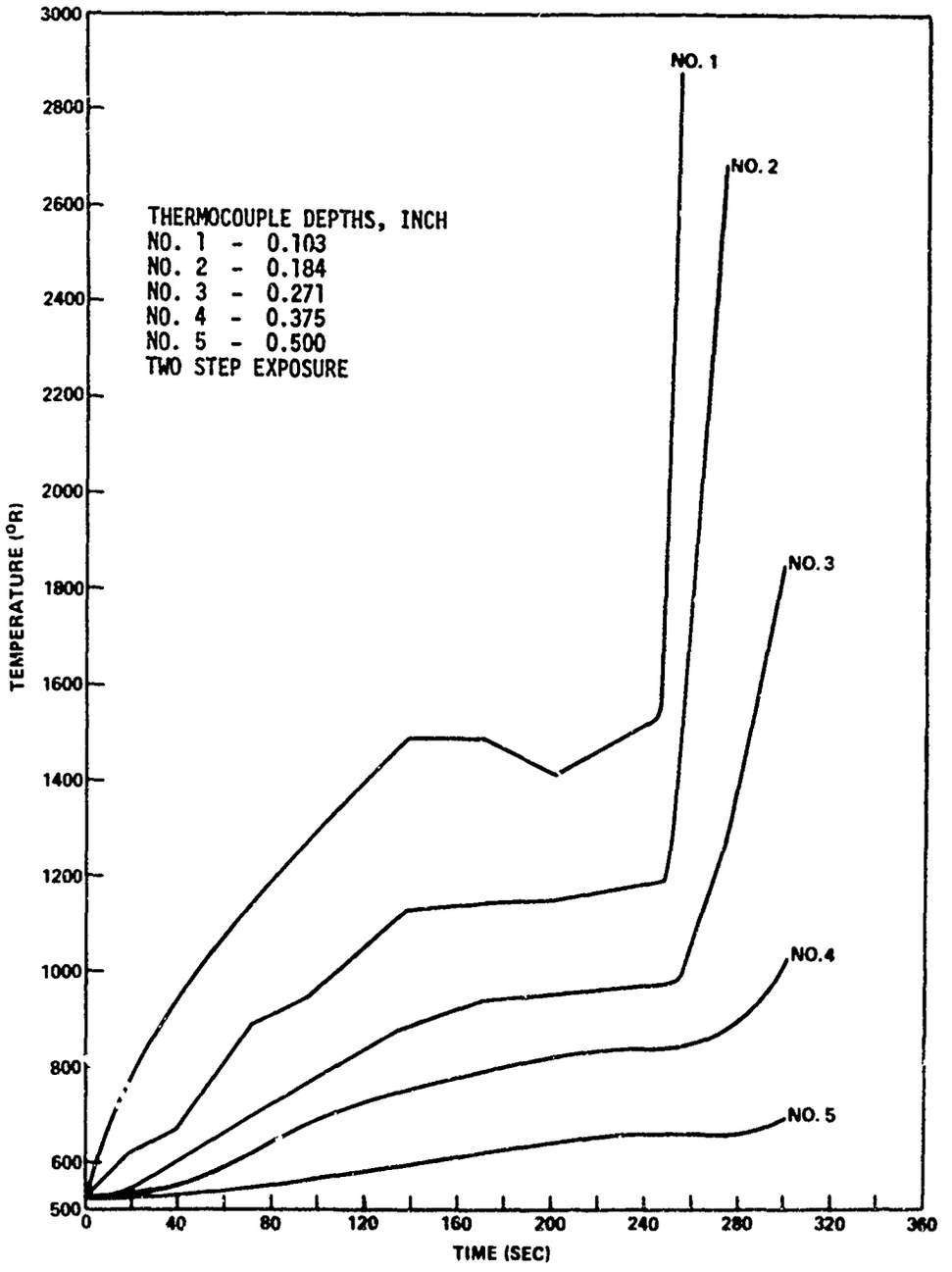

Figure 13. Internal Temperature Histories For R1 Silica Phenolic

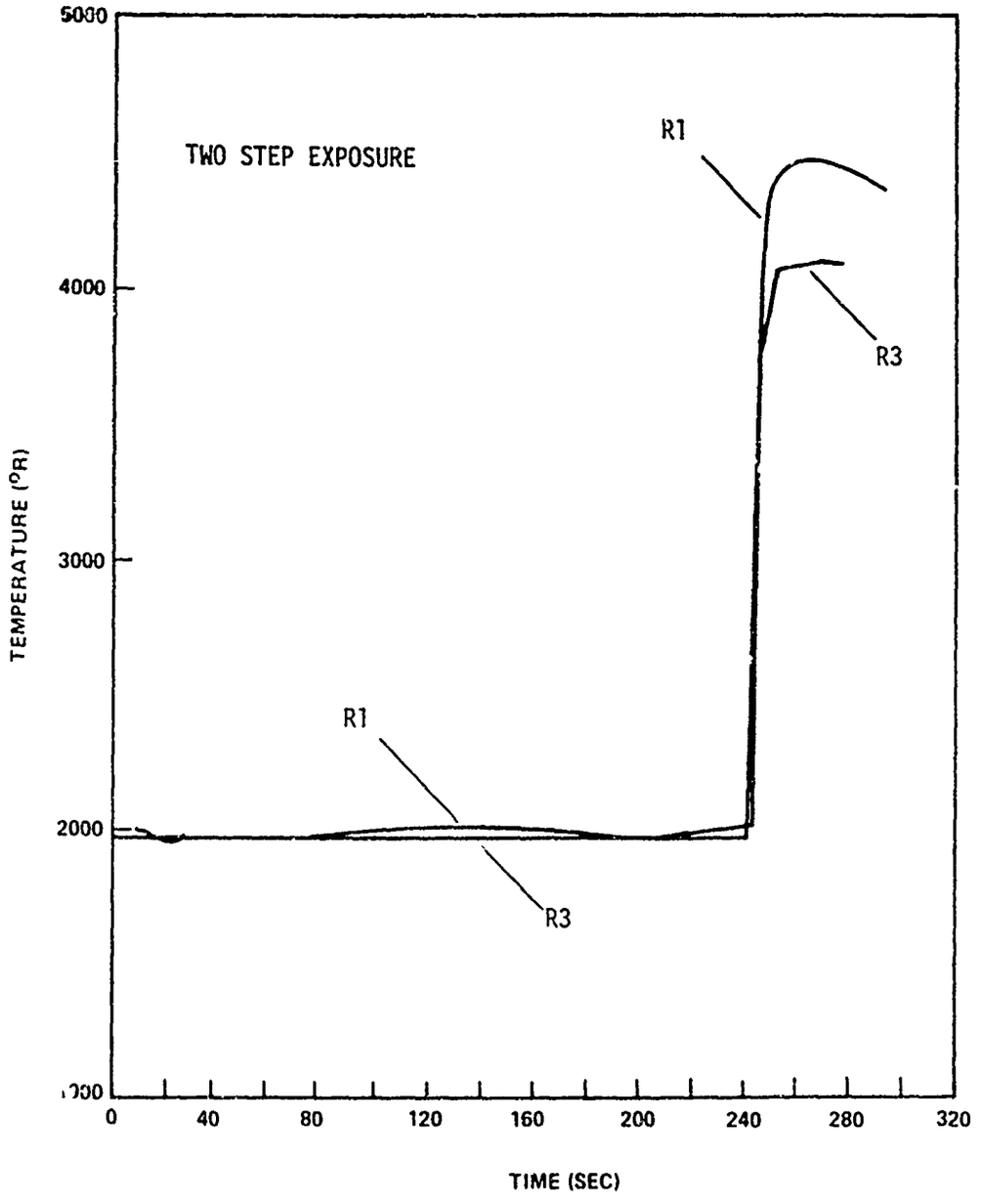

Figure 14. Surface Temperature History For Carbon Phenolic (R3) And Silica Phenolic (R1)

A calculated recession of 0.11 inches was essentially identical to the R3 mean value but high with respect to the R2 specimen (Figure 8, Table VI). The calculated char depth of 0.365 inches exceeded that found for both carbon-phenolic specimens (Figure 8, Table VI). The calculated recession histories were nearly linear for the two steps; the char histories were less linear reflecting the transient nature of the environment. Both cases were averaged to give mean linear values for step 1/step 2. The results were 0.00010/0.0016 inches/sec and 0.00092/0.0026 inch/sec for the recession rate and the charring rate, respectively.

The calculated internal temperatures were in fair agreement with results for the R2 run; there was considerable difference with respect to the R3 specimen (Figures 9, 10, and 15). The good agreement between the calculated and actual R3 recession as compared to the differences in in-depth charring and temperature could not be adequately explained. Two important aspects were an experimentally low heat flux for the R2 second step, which resulted in a low recession, and the irregular recession and charring for R3 (Table VI, Figure 8).

The calculated surface temperature history contained a first step transient that was not observed experimentally. The starting value of about 1000°R increased slowly, reaching the experimental level near 2000°R at about 160 seconds, and continued to increase on up to the step change. The differences between the calculated and experimental temperatures were less than a few hundred degrees for the second step. The calculated and measured temperature discrepancy for the first step was not readily resolvable.

The environmental parameter inputs to the code were a more accurate representation of the experimental case than the nominal values (Tables I and VI). The enthalpy was adjusted to 5500 and 4500 Btu/lb for the two steps. The heat fluxes involved 28 Btu/ft^2-sec and incremental levels of 360/320/340 Btu/ft^2-sec, respectively. These levels were based upon an average pressure history of 1 atm and increments of 0.82/0.82/0.88 atm for the first and second steps, respectively. A comparison was made

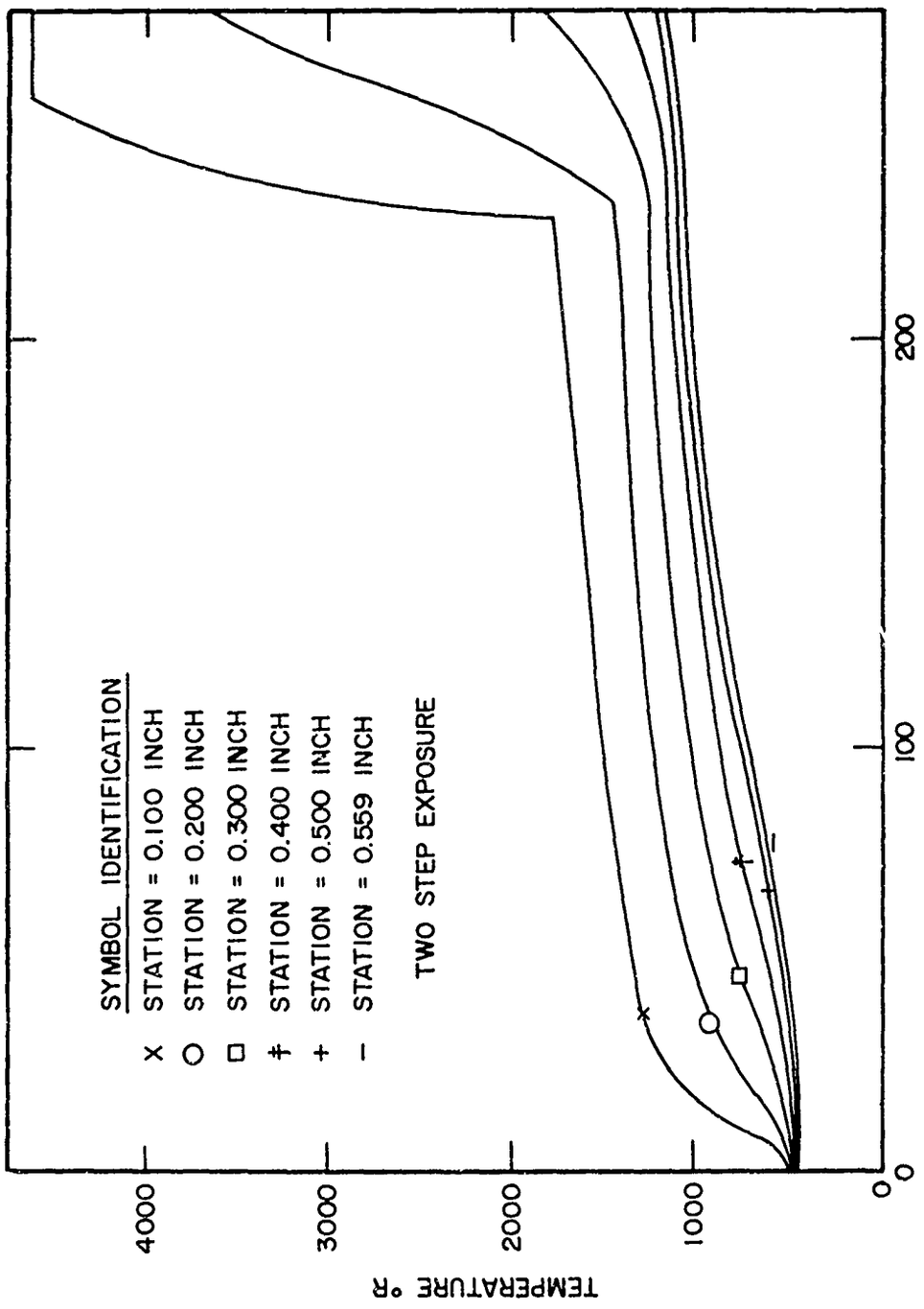

Figure 15. Predicted Internal Temperature History For Carbon Phenolic

between this and an earlier model with the single difference of a constant second step heat flux of 360 Btu/ft^2-sec. The refined model predicted less recession, more char, and a higher surface temperature for the second step. In addition, a saddle-like change in the surface temperature was found for the refined model but not for the first one. In terms of an experiment, this type of a break, which was observed for R2 and to a lesser degree for R1, appeared consistent with local pressure change resulting from erratic flow expansion, specimen and shock interactions, specimen ablation, or a combination of these effects.

Excluding the apparent normal ablative behavior resulting in some irregularity and porosity of the surface in conjunction with an uneven char layer, there were several experimental artifacts with the potential of contributing to these physical results. The experimental aspects were related to decreasing recession along the specimen during the first step, shock reflections and specimen interactions, downstream effects by ejected upstream contaminants, and heat losses in the nozzle region. Considering these factors, possible interactions, and variability with composite type, it was considered that the most reliable char and recession results corresponded to an average over the specimen mid-region.

Two R2 runs required termination due to equipment malfunctions. One run was ended during the first step; the second, just after bypass closure. The recession generally decreased along the specimen surface, an observation consistent with a low mass flow losing energy down the surface. Expansion was found at the downstream end of one specimen. The actual recession was apparently dependent upon undefined conditions resulting from the malfunction, which consisted of anode failure with water flooding in one case and failure of the bypass plug to seat properly in the second.

The char and recession variability along the length of the specimen was probably initiated during the first step. Uneven recession in the mid-region during the second step was consistent with but not necessarily

totally due to flow environmental changes. A decline in heat flux and enthalpy beyond the mid-region was the expected result of flow expansion in the rectangular nozzle.

The nozzle design condition was for expansion to atmospheric pressure at the exit to provide a parallel flow with minimum shock reflections and specimen interactions. Experimentally, specimen ablation frequently opened the channel and resulted in an exit pressure below atmospheric. The local ablative behavior changed with any significant reflections and interactions. A self-aggravating effect was possible. A technique to reduce underexpansion, an upstream pressure just above atmospheric, was not always feasible due to power control limitations and specimen ablation.

The ablative species generated and ejected into the flow in the upstream region contaminated the downstream flow. The seriousness of the contamination could not be readily resolved. For many specimens, there was some evidence of a heat loss effect in the nozzle region, a result of excessive conduction into the nozzle hardware.

A run was made for a specimen of graphite (ATJ-S). This material was expected to result in minimum flow perturbation due to the small total recession, to be relatively free of any shock interaction-induced local recession, and to give minimum downstream contamination. The initial thickness range was 0.581-0.614 inches,. the recession range was 0.017-0.045 inches, and the peak recession was found at a station 2 inches from the leading edge. There was an increase in total recession from the leading edge to the mid-region and then a decline from this area to the end of the specimen. The graphite results confirmed that irregular recession formed during the first step and that flow expansion effects during the second were viable mechanisms for the composites. Any accelerated recession resulting from shock interactions was considered strongly composite-type dependent. Flow contamination and nozzle heat loss effects were considered secondary to these other mechanisms. Therefore, it was concluded that the most error-free data should be taken as an average for the mid-region of the specimen.

The original air arc heater was modified with auxiliary hardware for this study. This effort required particular developmental emphasis for the bypass nozzle, the graphite plug for this nozzle, and the graphite specimen insulator.

2. MULTIPLE STEP EXPOSURES

R6 carbon phenolic specimens were exposed to multiples of a five step sequence of increasing and decreasing environmental parameters (Table VII). The objective of using sequential steps was to isolate early and late mechanisms and to measure specimen physical change and weight loss.

The mean recession rates, as measured by a photographic technique during the run, were not always consistent with the rise and fall of enthalpy and heat flux (Table VII). For the first and fifth steps, the film image was not bright enough for recession evaluation. The total recession and the total weight loss, as measured for a core taken at the reference station 1.5 inches from the leading edge, were generally consistent with the step changes in environmental parameters (Table V). This conclusion excluded the data for specimens 2, 6, and 7 due to malfunctions for these runs. The differences found between the areal weight change for the core and the total specimen were associated with irregular specimen charring and recession (Table V). The magnitude of the difference tended to follow the increasing and decreasing environmental parameters.

The internal temperature history data were scattered but not unreasonable (Figure 16). The general trend was for steadily increasing temperature with time, with some temporal changes in the rate, at the six thermocouple depths. Consistent with the largest increase in flow energy, the first step change resulted in the largest internal temperature perturbation.

TABLE VII

EXPERIMENTAL RESULTS - R6 C/P MULTIPLE STEP EXPOSURES

Item/Specimen Number	Step Number	1	2[a]	3[b]	4	5	6[c]	7[d]	8
Enthalpy, Btu/lb	1	1080	1010	1050	1150	1120			1050
	2		3520	3520	3690	3550			3520
	3		2340	5920	6190	5920	4060	5860	5920
	4					3830	1900	3890	3860
	5						1730	1790	1730
Heat Flux, Btu/sq ft-sec	1	229	213	220	241	234			220
	2		473	472	490	472			467
	3		263[a]	656	689	654	452[c]	651	654
	4					508	253[c]	517	512
	5						286	297	290
Time, sec	1	19.78	20.20	20.41	20.03	20.05			20.00
	2		14.65	15.00	14.73	14.95			15.00
	3		1.16[a]	8.23[b]	12.80	13.08	13.25	13.08	13.10
	4					16.20	16.05	16.43	15.38
	5						10.23	7.35[d]	21.05
Recession Rate, $(inch/sec) \times 10^{-4}$	1	--	--	--	--	--			--
	2		2.70	2.64	3.10	3.25			3.32
	3		--	2.81	3.10	3.25	2.25[c]	2.90	3.57
	4					5.45	--	4.34	5.57
	5						--	--	--
Surface Radiation, Btu/sq ft-sec	1	9	14	39	59	38			35
	2		197	179	209	189			193
	3		148[a]	313	465	408	174[c]	300	420
	4					312	105[c]	264	298
	5						111	154	86
Surface Temperature, °R	1	2460	2490	3330	3640	3240			3230
	2		4890	4850	4980	4920			4900
	3		4260[a]	5650	6230	6060	4930[c]	5500	6050
	4					5600	4300[c]	5250	5430
	5						4370	4500	3960

[a]Step 3: terminated early manually; heat flux probably erroneous. Transient surface radiation and temperature values. [c]Step 3: terminated early manually. Specimen data for re-exposure to steps 2 and 3. [c]Steps 3, 4: arc arc failed; heat flux and specimen 1 is probably erroneous. [d]Step 5: terminated early manually. "--" denotes image obtained because of cracked film; no recession rate data.

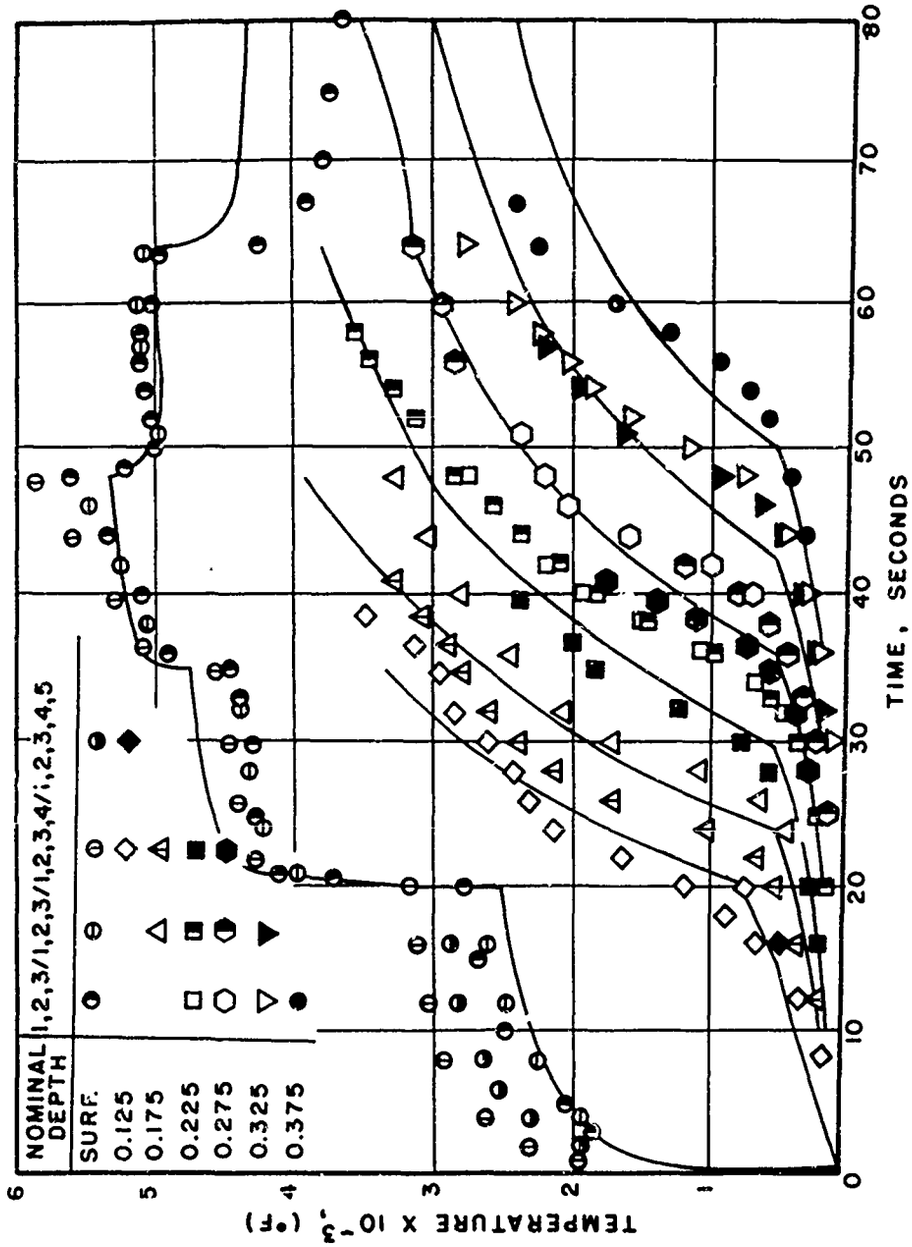

Figure 16. Internal And Surface Temperature Histories For R6 Carbon Phenolic

The more distinctive response features for the five steps included the following:

Step 1. An expanded and thin char beneath a roughened surface with little actual recession. The cloth edges were distinctly exposed. The surface radiation and temperature was not reproducible from run to run. The irregular behavior was tentatively attributed to surface kinetics control of char oxidation and the known kinetic dependences upon surface characteristics in this regime.

Step 2. A thicker char with the onset of recession at a rate of about 0.003 inch/sec. The surface temperature was relatively reproducible for the different runs.

Step 3. The recession rate was essentially the same as for step 2 for this peak heating condition. The exact reasons were not clear. The apparently real recession could have been associated with a constant oxidative mechanism or an error in the measurement of a transient rate.

Step 4 An unexpectedly high recession for the heating rate. The high-speed surface movies showed an onset appearance of fine-scale micromechanical removal of particles of apparently weakened char.

Step 5. The estimated recession rate was 0.006 inch/sec, a value higher than for step 4. There was film evidence of increased particle loss in a milder environment. The surface temperature was low, a result consistent with a micromechanical removal mechanism.

Steps 3, 4 and 5. This sequence was run to establish if micromechanical removal effects were inherent for the composite and/or dependent upon prolonged heating under steps 1 and 2. Neither the step simulation nor the experimental data were satisfactory. For specimen 7, the recession rate was lower than for specimens with pre-heating under steps 1 and 2. The movies, however, revealed a low rate of micromechanical removal, a result consistent with the lower than expected surface temperatures for this run.

All Steps. The reduction of convective heat flux resulting from surface radiation was approximately 20%, 40%, 65%, 60%, and 30% for steps 1 through 5, respectively.

The response of the R6 composite to the five step sequence was predicted by means of a charring-ablator computer code. The principal thermophysical properties were obtained for a R6 specimen by a nonlinear regression analysis of data for a test in a steady-state environment (Table IV). The nominal values of the environmental parameters were used as inputs (Table I).

The calculated recession showed two regions of disagreement with respect to the experimental results (Figure 17). A slightly high recession predicted for steps 1, 2, and 3 was tentatively attributed to use of a diffusion-control limit on recession in the simplified computer code rather than modelling surface kinetics control. A high recession observed for step 4 and as extrapolated to step 5 was an apparent result of micromechanical surface removal.

The calculated in-depth temperature histories were generally consistent with the experimental results with respect to magnitude and relative shape (Figure 16). There was generally an increase in the rate of temperature rise between 500° and 1200°F. This effect was consistent with and possibly due to endothermic resin pyrolysis and a reduction in local thermal conductivity. The gradual decrease in the rate at higher temperatures was consistent with a possible increase in char thermal conductivity. The experimental rates increased more rapidly at later times than the calculated values, a potential result of micromechanical surface removal.

The predicted surface temperatures were low for steps 1 and 2. This was partially due to improper representation of oxidative reactions for the computer model. The agreement between calculated and experimental values was reasonable for steps 2 and 3. The low experimental results for step 5 were associated with the micromechanical removal mechanism.

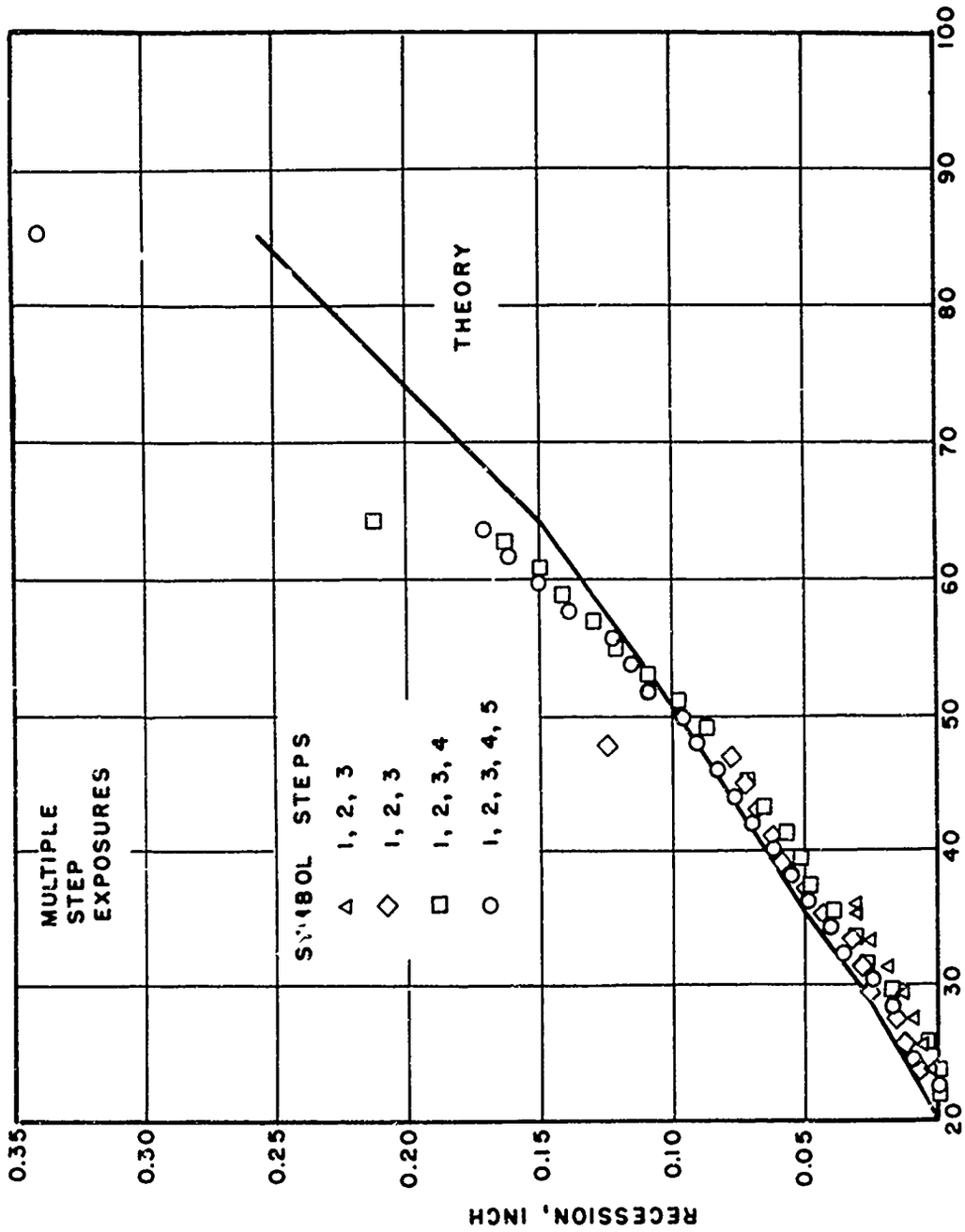

Figure 17. Surface Recession For R6 Carbon Phenolic

The multiple step specimens underwent irregular charring and recession with the relative severity increasing with the number of steps. The more reliable ablative information corresponded to the specimen mid-region. The physical measurements were made at the reference station in this area. Based upon the analysis of two step exposures, it was considered that the most important sources of irregular recession involved initiation during early heating and flow expansion effects with some contribution by nozzle heat losses.

SECTION VI

SUMMARY AND CONCLUSIONS

An investigation was made of the fundamental response of carbon phenolic and silica phenolic composites under extended heating conditions. Specimens were characterized under stepwise heating pulses of either five minutes (two steps) or up to 1.4 minutes (to five steps) in duration.

The response under two step heating was dependent upon composite type. Considering the influence of artifacts associated with environmental/specimen interactions, the internal and surface temperatures, recession rates, and surface recession patterns were not unreasonably anomalous for one each carbon phenolic and silica phenolic composite.

The agreement of charring-ablator predictions for a nominal carbon phenolic in a nominal two step environment with experimental results was dependent upon composite type and the specific test. There was no direct evidence of micromechanical removal of the surface for this low shear environment.

The ablation of carbon phenolic under a five step heating sequence consisted of thermochemical and thermomechanical mechanisms. The char surface was lost by conventional oxidative mechanisms including surface kinetics control at low temperatures. There was micromechanical surface removal under sufficiently severe heating, an effect dependent to some degree upon prolonged early heating. The computer code analysis of response was in fair agreement with experimental results consistent with the code modelling of oxidative mechanisms, the exclusion of micromechanical mechanisms from the code, and the uncertainty in environmental and property inputs.

SECTION VII

RECOMMENDATIONS FOR FUTURE STUDY

The study revealed several deficiencies in securing accurate and useful analytical and experimental results. Specific areas of needed improvement included:

a. Accurate control and reproducibility of environmental variables including the monitoring of the variables during the run.

b. Increased accuracy in the measurement of the environmental variables.

c. Statistical characterization of a material to determine mean response data.

d. Careful apparatus design with a view toward suppressing heat and mass transfer errors. Examples include: continuous specimen repositioning to avoid flow perturbations; minimal flow contamination; minimal shock wave/specimen interactions; optimal channel nozzle design to minimize flow expansion effects; specimen insulation against edge and nozzle heat losses; uniform heat and mass transfer along the specimen.

e. Multiple station monitoring of specimen recession rate and surface temperature.

f. Heat flux and pressure diagnostics for shapes simulating specimen recession patterns.

g. An accurately modelled computer code for response analysis including micromechanical removal modes.

h. Accurate thermophysical properties for the material.